Neurobiology of Aging 74 (2019) 21–37

Contents lists available at ScienceDirect

Neurobiology of Aging

journal homepage: www.elsevier.com/locate/neuaging

Functional signature of conversion of patients with mild cognitive impairment

Stefano Delli Pizzi [a,b], Miriam Punzi [a,b], Stefano L. Sensi [a,b,c,*], for the Alzheimer's Disease Neuroimaging Initiative [1]

[a] Department of Neuroscience, Imaging and Clinical Sciences, "G. d'Annunzio" University, Chieti, Italy
[b] Center for excellence on Aging and Translational Medicine - Ce.S.I. - Me.T., "G. d'Annunzio" University, Chieti, Italy
[c] Departments of Neurology and Pharmacology, Institute for Memory Impairments and Neurological Disorders, University of California-Irvine, Irvine, CA, USA

ARTICLE INFO

Article history:
Received 1 April 2018
Received in revised form 24 September 2018
Accepted 4 October 2018
Available online 12 October 2018

Keywords:
Alzheimer's disease
Cerebellum
entorhinal cortex
functional connectivity
Hippocampus
GABA
Excitotoxicity

ABSTRACT

The entorhinal-hippocampal circuit is a strategic hub for cognition and the first site affected by Alzheimer's disease (AD). We investigated magnetic resonance imaging patterns of brain atrophy and functional connectivity in an Alzheimer's Disease Neuroimaging Initiative data set that included healthy controls, mild cognitive impairment (MCI), and patients with AD. Individuals with MCI were clinically evaluated 24 months after the first magnetic resonance imaging scan, and the cohort subdivided into sets of individuals who either did or did not convert to AD. The MCI group was also divided into patients who did show or not the presence of AD-related alterations in the cerebrospinal fluid. Patients with AD exhibited the collapse of the long-range hippocampal/entorhinal connectivity, pronounced cortical/subcortical atrophy, and a dramatic decline in cognitive performances. Patients with MCI who converted to AD or patients with MCI who showed the presence of AD-related alterations in the cerebrospinal fluid showed memory deficits, entorhinal/hippocampal hypoconnectivity, and concomitant atrophy of the two regions. Patients with MCI who did not convert to AD or patients with MCI who did not show the presence of AD-related alterations in the cerebrospinal fluid had no atrophy but showed hippocampal/entorhinal hyperconnectivity with selected neocortical/subcortical regions involved in memory processing and brain metastability. This hyperconnectivity may represent a compensatory strategy against the progression of cognitive impairment.

1. Introduction

Brain aging and aging-related neurodegenerative disorders are a significant health challenge for contemporary societies. Brain aging represents a favorable background for the onset and development of neurodegeneration and dementia. Alzheimer's disease (AD) is a condition associated with the development of irreversible cognitive and behavioral deficits and preceded by a prodromal stage known as mild cognitive impairment (MCI). Patients with MCI do not fulfill the diagnostic criteria for dementia but show significant cognitive deficits that mostly occur in mnemonic domains (Petersen et al., 2010). Patients with MCI progress to AD in 60%–65% of cases (Busse et al., 2006) with a conversion rate that reaches 8.1% per year (Mitchell and Shiri-Feshki, 2009). Thus, the early identification of the brain changes associated with MCI is critical to catch the disease at its initial stage, unravel its pathogenic mechanisms, and help the design of more effective therapeutic interventions.

Neuroimaging approaches have been extensively used to detect the initial changes associated with the early stages of AD (Frisoni and Jessen, 2018). Resting-state functional magnetic resonance imaging (rs-fMRI) is a noninvasive tool that allows the investigation of the operational changes and network reconfigurations that occur in several neurological/neurodegenerative conditions, including AD. In patients with MCI, rs-fMRI has been successfully used in the quest to detect abnormalities in the brain functional connectivity that occur before the appearance of patent signs of structural damage (Badhwar et al., 2017; Canuet et al., 2015; Drzezga et al., 2011).

* Corresponding author at: Molecular Neurology Unit Center of Excellence on Aging and Translational Medicine (CeSI-MeT) University "G. d'Annunzio", Chieti-Pescara Via Luigi Polacchi 11, Chieti 66100, Italy. Tel.: +39 0871 541544; fax: +39 0871 541542.
E-mail address: ssensi@uci.edu (S.L. Sensi).

[1] Data used in the preparation of this article were obtained from the Alzheimer's Disease Neuroimaging Initiative (ADNI) database (adni.loni.usc.edu). As such, the investigators within the ADNI contributed to the design and implementation of ADNI and/or provided data but did not participate in analysis or writing of this report. A complete listing of ADNI investigators can be found at: http://adni.loni.usc.edu/wp-content/uploads/how_to_apply/ADNI_Acknowledgement_List.pdf.

0197-4580/$ – see front matter © 2018 Elsevier Inc. All rights reserved.
https://doi.org/10.1016/j.neurobiolaging.2018.10.004

The entorhinal-hippocampal circuit is a strategic region for the control of cognitive processes and the first site to be affected by the AD-related pathology (Braak et al., 2013; Gomez-Isla et al., 1996). In the AD brain, early signs of synaptic degradation occur within the perforant path, neurodegeneration then spreads to the layers II-III of the entorhinal cortex, the hippocampal CA1 subfield, the subicular areas, ultimately affecting the whole hippocampus (Mueller et al., 2010; Wolk et al., 2011; Yushkevich et al., 2015). This sequence is crucial as the entorhinal-hippocampal complex plays an essential role in the processing of long-term memory (Preston and Eichenbaum, 2013). Functional changes in the hippocampus and, in particular, the CA3/dentate regions have been associated with the occurrence of episodic memory deficits that develop upon physiological aging and MCI (Yassa et al., 2010a, 2011). Moreover, the hippocampus plays a role in maintaining the brain system stability and promotes the adaptive recalibration of network functioning observed in response to pathological stressors (Hillary and Grafman, 2017; van den Heuvel and Sporns, 2011).

In this study, we investigated, in a cohort of 135 individuals, differences in structural MRI (sMRI) and rs-fMRI features that occur within the corticohippocampal and corticoentorhinal circuits. The study group included healthy controls (HCs) (n = 40), patients with MCI (n = 67), and patients with AD (n = 28). The data set also provided information on the demographic, neuropsychological/clinical, apolipoprotein E (APOE) status, and the cerebrospinal fluid (CSF) levels of AD-related pathogenic proteins like the amyloid β_{1-42} peptide ($A\beta_{1-42}$), tau phosphorylated at threonine 181 (p-Tau_{181}), and the ratio of p-$Tau_{181}/A\beta_{1-42}$.

sMRI data were used to investigate differences in brain volumes and cortical thickness among the study participants. rs-fMRI data were used to evaluate differences in the functional connectivity (FC) occurring in the circuits linking the hippocampus or the entorhinal cortex to the cortex. The progression or clinical stability of HC or patients with MCI was assessed by using clinical follow-up data obtained 24 months after the initial MRI session. These longitudinal data were instrumental to divide the MCI group into two subsets: patients who converted (c-MCI) or did not convert (nc-MCI) to AD. As not all the MCI symptoms are necessarily dependent on the presence on underlying AD pathology, it is conceivable that some nc-MCI patients are protected from the AD conversion mainly because of the absence of significant levels of amyloid- or tau-related pathology. Conversely, compared to MCI with low levels of amyloid and tau, patients with MCI with high levels of these molecular AD determinants are likely to convert with higher frequency (Jack et al., 2016; Johnson et al., 2016). Thus, to explore this issue, in a subsequent analysis, we also subdivided our MCI sample in patients with MCI who showed the presence of AD-related alterations in the cerebrospinal fluid (MCI^{AD+}) or patients with MCI who did not show the presence of AD-related alterations in the cerebrospinal fluid (MCI^{AD-}) by taking in consideration the presence of an AD-related CSF biomarker, the p-$Tau_{181}/A\beta_{1-42}$ ratio, a value that can be used as a proxy of ongoing pathology.

The overall aim of the study was to unravel a functional biomarker, centered on the FC of the hippocampus and entorhinal cortex that can be used to identify patients with MCI who are more likely to convert to AD. As altered synaptic activation and plasticity participate in shaping the course of the disease, we tested whether nc-MCI patients, among other factors, maintain their cognitive status through an underlying adaptive hyperconnectivity that takes place between the hippocampus and the neocortical/subcortical regions that are strategic for memory processing and brain metastability. We also tested whether c-MCI and patients with AD diverge from nc-MCI in terms of structural and functional changes that correlate with the decline of the cognitive performances. Finally, given the role of amyloid and tau-driven pathology in the modulation of neurodegeneration, we also evaluated how the presence of these proxy indices of AD-related pathology affect the connectivity patterns of the MCI^{AD+} and MCI^{AD-} subgroups.

2. Materials and methods

2.1. Experimental design

Data used for this article were obtained from the Alzheimer's Disease Neuroimaging Initiative (ADNI)-GO/2 database. ADNI was launched in 2003 as a public-private partnership led by Michael W. Weiner. The primary goal of ADNI is to use serial MRI, positron emission tomography (PET), biological markers, and clinical and neuropsychological data to investigate the features of patients affected by the AD spectrum. For up-to-date information on the initiative, see www.adni-info.org.

Experiments fulfilled the ethical standards and the Declaration of Helsinki (1997) and subsequent revisions. Informed consent was obtained from study participants or authorized representatives. Study participants had a good general health status and no diseases expected to interfere with the study. Overall, the ADNI-GO/2 database included 170 participants who have completed the 3T-sMRI and 3T-rs-fMRI. The age range was between 57 and 88 years.

Participants who did not complete a clinical follow-up, performed 24 months after the first MRI session, or those who showed the presence of technical issues related to their MRI raw data (i.e., artifacts, dishomogeneity in acquisition parameters, images deformed for missing information raw file) were excluded from the study sample (Supplementary Fig. 1). Our final sample included 135 participants divided into 40 HCs, 67 patients with MCI, and 28 patients with AD. Based on the clinical follow-up, the MCI group was further subdivided into a group of 54 nc-MCI patients and 13 c-MCI patients. Our MCI sample was also subcategorized taking into account the CSF levels of AD-related biomarkers. Using a cutoff of 0.0198 for the p-$Tau_{181}/A\beta_{1-42}$ ratio (Schindler et al., 2018), the MCI group and the nc-MCI subset was divided into patients positive [MCI^{AD+}(n = 37) or nc-MCI^{AD+}(n = 25)] or negative [MCI^{AD-} (n = 22) or nc-MCI^{AD-}(n = 21)] for AD pathology (Supplementary Fig. 2).

2.2. Neuropsychological assessment

All patients underwent clinical and cognitive evaluations at the time of the MRI scan. The ADNI neuropsychological data set includes the Mini-Mental State Examination (MMSE) (Folstein et al., 1975) and the Montreal Cognitive Assessment (Nasreddine et al., 2005) to investigate global cognition; the Functional Activities Questionnaire for the assessment of daily living activities (Pfeffer et al., 1982); the Alzheimer's Disease Assessment Scale-Cognitive subscales (ADAS-11 items scores; ADAS-13 items scores) to evaluate the severity of impairments of memory, learning, language (production and comprehension), praxis, and orientation (Mohs and Cohen, 1988; Mohs et al., 1997); the Animal Fluency (Morris et al., 1989) and the 30-item Boston Naming Test (Kaplan and weintraub, 1983) to investigate semantic memory and language abilities; the Trail Making Test, part A and B (time to completion) to assess attention/executive functions (Spreen, 1998); the Rey Auditory Verbal Learning Test and Logical Memory II, subscale of the Wechsler Memory Scale-Revised (WMS-R) to investigate recall and recognition (Rey, 1964; Wechsler, 1987).

HCs were free of memory complaints and without significant impairment as far as general cognitive functions or performance in daily living activities. The inclusion criteria for HCs were MMSE scores between 24 and 30, a global score of 0 on the Clinical Dementia Rating Scale (CDR-RS; Morris, 1993), and a score above the cutoff level on the WMS-R Logical Memory II (≥3 for 0–7 years of

education, ≥5 for 8–15 years of education, and ≥9 for 16 or more years of education).

The inclusion criteria for patients with MCI were MMSE scores between 24 and 30, memory impairments identified by the partner, with or without complaints by the participant, a CDR-RS score of 0.5, and memory deficits as indicated by scores below the cutoff level on the WMS-R Logical Memory II (3–6 for years of education 0–7, 5–9 for 8–15 years of education, and ≤9 for >15 years of education). The subject general cognition status and functional performances were sufficiently preserved to exclude a diagnosis of AD.

Patients with AD fulfilled the criteria of probable AD set by the National Institute of Neurologic and Communicative Disorders and Stroke as well as the Alzheimer's Disease and Related Disorders Association. Patients with AD had MMSE scores between 20 and 26 and CDR-RS scores between 0.5 and 1.0.

2.3. CSF and APOE genotyping

CSF data were available for 87.4% of the total sample. The set included information on levels of the $A\beta_{1-42}$, total tau (t-Tau), and p-Tau_{181}. Highly standardized $A\beta_{1-42}$, t-Tau, and p-Tau_{181} levels were measured using the Roche automated immunoassay platform (Cobas e601) and immunoassay reagents. Details on the methods for the acquisition and measurement of CSF are reported in the ADNI website (http://www.adni-info.org). The APOE ε4 allele frequency was also investigated at the screening stage.

2.4. MRI acquisition protocol

MRI data were all acquired with a Philips 3T scanner (see details at http://adni.loni.usc.edu/wp-content/uploads/2010/05/ADNI2_MRI_Training_Manual_FINAL.pdf), thereby limiting bias and technical issues associated with the use of different scanner types/brands. T_1-weighted images were obtained using 3D Turbo Field-Echo sequences (slice thickness = 1.2 mm; repetition time/echo time = 6.8/3.1 ms). One run of resting-state Blood Oxygen Level Dependent fMRI data were acquired using gradient-echo T2*-weighted echo-planar imaging (EPI) sequence (in-plane voxel size = 3.3125 mm × 3.3125 mm; slice thickness 3.3125 mm; repetition time/echo time = 3000/13 ms. Patients were instructed to lay still and keep their eyes open during acquisition.

2.5. MRI data analysis

FreeSurfer (version 6.0) was used to perform sMRI and rs-fMRI data analysis. For each study participants, T_1-weighted images were analyzed using the "recon-all-all" command line to obtain the automated reconstruction and labeling of cortical and subcortical regions (Fischl et al., 2004). The preprocessing steps encompassed magnetic field inhomogeneity correction, affine-registration to Talairach Atlas, intensity normalization, and skull-strip. The processing steps involved segmentation of the subcortical white matter (WM) and deep gray matter (GM) volumetric regions, tessellation of the GM and WM matter boundary, automated topology correction, surface deformation following intensity gradients to optimally position the GM and WM and GM/CSF borders at the location where the greatest shift in intensity delineates the transition to the other tissue class. The total volume of the left and right hippocampi and the estimated total intracranial volume (eTIV) were calculated using the "asegstats2table." The hippocampal volumes were normalized with a ratio obtained by dividing hippocampal volumes by eTIV. The left and right masks of the hippocampi and entorhinal cortices were obtained by the "recon-all -all" command lines and used as "seed regions" for FC analysis using FreeSurfer–Functional Analysis Stream (http://surfer.nmr.mgh.harvard.edu/fswiki/FsFastFunctionalConnectivityWalkthrough). The "preproc-sess" command line was used to perform motion and slice timing corrections, masking, registration to the structural image, sampling to the surface, surface smoothing by 5 mm, and sampling to the MNI305 with volume smoothing. Surface sampling of time-series data was carried out onto the surface of the left and right hemispheres of the "fsaverage" template of FreeSurfer. Nuisance regressors were obtained for each study participants by extracting the EPI average time courses within the ventricle mask and the WM mask (taking into consideration the top 5 principal components). These regressors and the motion correction parameters were eliminated from the EPI time series. Temporal band-pass filtering ($0.01 < Hz < 0.1$) was applied to analyze only rs-fMRI data within this frequency range. The first four rs-fMRI time points were discarded to allow T_1-weighted equilibration of the MRI signal. The mean signal time course within each seed region was used as "regressor" to assess FC. With the "selxavg3-sess" command line, we performed the first-level analysis (single-subject analysis) including the computation of the Pearson correlation coefficient (r-value) between the time series within the seed and the time series at each voxel. The obtained correlation maps were then converted to Z-score maps before entering the second-level analysis (group analysis). The "isxconcat-sess" command line was used to create a "stack" of maps from each patient.

The Desikan-Killiany Atlas (Desikan et al., 2006) was used to identify the location of clusters displaying sMRI differences. In addition, two functional atlases focused on cortical (Yeo et al., 2011) and cerebellar (Buckner et al., 2011) networks were used to integrate the information provided by the Desikan-Killiany Atlas and define the positioning of clusters that show between-group differences or within-group correlations. Mean thickness and z-scores were extracted from each region of interest by using the "mri_segstats" and "mris_anatomical_stats" command lines.

For each patient, we have performed pair-wise correlations of the time series obtained, in the right and left hemispheres, in the hippocampus, and the entorhinal cortex. Using the Fisher transformation, Pearson's R-values were transformed into a t-value and entered into (1) one sample t-test to assess whether the connectivity values are significantly greater than zero within each group; (2) analysis of variances to assess between-group differences.

2.6. Statistical analysis

One-way analysis of variance and Bonferroni post hoc test were used to evaluate the group differences regarding demographic/clinical data and the hippocampal and entorhinal morphometry. Chi-squared test was used to investigate the group differences on gender and the APOE ε4 carrier status. For analyses related to FC and cortical thickness, general linear models (https://surfer.nmr.mgh.harvard.edu/fswiki/FsgdFormat) were used. The study investigated the differences between groups. The first comparison was HCs, nc-MCI patients, c-MCI patients, patients with AD; the second comparison was HCs, MCI^{AD-} patients, MCI^{AD+} patients, patients with AD; the third comparison was HCs, nc-MCI^{AD-} patients, nc-MCI^{AD+} patients, patients with AD. Moreover, further general linear models were used, in the MCI patients, to assess, relationships between FC strength and other variables of interest like the seed morphometric measures, the cortical thickness in each vertex, and CSF biomarkers. The correlation analyses between the variables of interest and the FC of a given seed region FC were performed in a vertex-by-vertex computation by using the "pvr" option in "mri_glmfit" and regressing out the effect of age and educational level. Using the "mri_concat" command line, conjunction maps were created to highlight the sites of overlaps occurring between

clusters expressing significant group difference and clusters that indicate significant correlations between FC strength and variables of interest. To investigate the effect of gender on FC, we took into consideration an additional model with two levels (male and female) and three variables including CSF biomarker levels, age, and educational levels. All the results are shown on statistical maps and adjusted by applying a clusterwise correction for multiple comparisons (Hagler et al., 2006). Finally, Spearman's correlation or "mri_glmfit" with mask (GM of the cerebellum) option was used, respectively, to investigate whether the hippocampal FC with the medial prefrontal cortex (mPFC) or cerebellum was associated with the longitudinal changes in neuropsychological test scores. Longitudinal variations were calculated as the Δ between baseline scores and scores at 24 months. Therefore, patients with MCI with smaller Δ are characterized by better longitudinal preservation of cognitive functions. All statistical tests were two-tailed, and the significant *p*-value threshold was set at 0.05.

3. Results

3.1. Demographic and clinical features of the study groups

When compared to HCs, global cognition and episodic memory (recall and recognition) were affected in MCI subsets and AD groups. Patients with AD also showed significantly higher frequency of APOE ε4 when compared to nc-MCI patients or HCs. Within the MCI subsets, global cognition and episodic memory (recall) were found to be more compromised in the c-MCI and MCI^{AD+} subsets. Between MCI subsets, no differences were found when considering other neuropsychological and clinical features or the APOE ε4 frequency. Patients with AD show altered levels of $A\beta_{1-42}$, t-Tau and p-Tau_{181} when compared to HCs. No statistically significant differences were found when comparing levels of CSF biomarkers in HCs versus nc-MCI or c-MCI versus AD. Higher levels of t-Tau, p-Tau_{181}, $A\beta_{1-42}$/t-Tau, and p-Tau_{181}/$A\beta_{1-42}$ as well as lower $A\beta_{1-42}$ concentrations were found in c-MCI patients when compared to HCs and in patients with AD compared to nc-MCI patients or HCs. No differences regarding age and educational levels were observed among the study groups (HC, MCI, and AD) or within the MCI subsets (nc-MCI and c-MCI or MCI^{AD-} and MCI^{AD+}). Statistics on demographics and clinical features of the study groups are shown in Tables 1–3 and Supplementary Tables 1 and 2.

3.2. Morphometric variations in the study groups

Compared to HCs or nc-MCI patients, patients with AD showed bilateral hippocampal and entorhinal atrophy. No differences in hippocampal volume or entorhinal thickness were found when comparing patients with AD with c-MCI. No statistically significant differences in hippocampal volumes were found in the comparison between the nc-MCI and HC subgroups. However, when compared to HCs, c-MCI patients exhibited signs of atrophy in the right hippocampus and the entorhinal cortex. Entorhinal atrophy in the right hemisphere was also found when comparing c-MCI with nc-MCI patients. When compared to HCs or MCI^{AD-} patients, MCI^{AD+} patients exhibited atrophy of the hippocampus. No differences in thickness of the entorhinal cortex were found when comparing MCI^{AD-} versus MCI^{AD+} patients or the two MCI groups with HCs. No differences in the eTIV were seen in the study groups. The statistical analysis of the structural data is shown in Tables 1 and 2 and Supplementary Table 1.

The comparison of patients with AD with nc-MCI patients (Supplementary Fig. 3A) or HCs (Supplementary Fig. 3C) revealed that the AD group shows a greater thinning of brain regions that belong to the default-mode network (DMN) and posterior memory network (PMN). A significant thinning of the mesial temporal areas was instead found in patients with AD when compared to c-MCI patients (Supplementary Fig. 3B). Finally, no statistically significant differences in cortical thickness were found when comparing c-MCI with nc-MCI patients or HCs. A region of interest–based analysis confirmed these surface-based results (Supplementary Table 3).

No statistically significant differences in cortical thickness were found when comparing HC versus MCI^{AD-}, HC versus MCI^{AD+} or MCI^{AD-} versus MCI^{AD+}. The comparison of patients with AD with MCI^{AD-} (Supplementary Fig. 4A) or MCI^{AD+} patients (Supplementary Fig. 4B) revealed that individuals with AD show a greater thinning of brain regions that belong to the DMN/PMN and the Salience Network (SN)/Cingolo-Opercular Network (CON). These changes were more patent in the AD versus MCI^{AD-} comparison. Compared to MCI^{AD-} patients, patients with AD displayed signs of atrophy in the mPFC and the superior parietal gyrus.

3.3. Hippocampal FC variations in subsets of MCI patients

The analysis of the hippocampal FC of MCI subgroups identified the presence of significant differences. First, we evaluated nc-MCI and c-MCI patients. Compared to HCs, nc-MCI patients showed enhanced FC between the hippocampus and the mPFC as well as the cerebellar regions that are part of DMN, the thalamus, and the striatum. The analysis also indicated reduced FC between the hippocampus and the brainstem (Fig. 1A). c-MCI patients showed hypoconnectivity of the hippocampus with the thalamus or the cerebellar areas that are part of the DMN and dorsal attention network and no differences in hippocampal FC with the rest of the cortex (Fig. 1B). Finally, the direct comparison within the nc/c MCI subset revealed that nc-MCI patients show hyperconnectivity between the hippocampus and the cerebellar areas that are functionally associated with the DMN, the SN/CON as well as the limbic system (Fig. 1C). Compared to nc-MCI patients, patients with AD showed diffuse patterns of hypoconnectivity between the hippocampus and cortical and cerebellar regions that are mainly involved in the DMN/PMN, the thalamus, or the brainstem. The hippocampus was also hypoconnected with the insula and sensorimotor regions as well as with cerebellar areas that are part of the limbic system (Fig. 2A). No significant differences were found by comparing c-MCI and AD groups. When compared to HCs, patients with AD showed decreased FC between the hippocampus and cortical and cerebellar regions that are part of the DMN/PMN, the striatum, and the brainstem. Moreover, hypoconnectivity of the hippocampus was observed with cerebellar regions of sensorimotor networks (Fig. 2B).

We also analyzed patients with MCI taking into account their load of AD-related pathology as expressed by altered values of an AD-related biomarker, the p-Tau_{181}/$A\beta_{1-42}$ ratio. Compared to HCs, MCI^{AD-} individuals exhibited hippocampal hyperconnectivity with the mPFC, the cortical and cerebellar regions that are part of the DMN, the amygdala, the hypothalamus, the striatum, and the thalamus (Fig. 3A). On the other hand, MCI^{AD+} individuals showed no differences in hippocampal FC with the cortex, but hypoconnectivity with cerebellar regions that are part of the DMN. We also found mixed patterns of hypoconnectivity/hyperconnectivity with cerebellar regions that are part of the frontoparietal network (FPN) and hyperconnectivity with cerebellar regions that are functionally linked to the limbic system (Fig. 3B). The MCI^{AD-} versus MCI^{AD+} comparison revealed that MCI^{AD-} patients show hippocampal hyperconnectivity with cortical and cerebellar regions that participate in the DMN and with the amygdala, the striatum, and the thalamus (Fig. 3C). Compared to MCI^{AD-} patients, patients with AD showed diffuse patterns of hippocampal hypoconnectivity with DMN/PMN- and SN-related cortical areas as well as with the brainstem, the hypothalamus, the thalamus, the limbic

Table 1
Demographic, neuropsychological, and clinical features—I model

Variable	Nc-MCI (N = 54)	c-MCI (N = 13)	ANOVA[d]		Post hoc					
			F or μ_2	*p*-value	HC vs. nc-MCI	HC vs. c-MCI	nc-MCI vs. c-MCI	nc-MCI vs. AD	c-MCI vs. AD	HC vs. AD
Gender (% Male)	54%	69%	8.729	**0.021**	**0.011**	**0.007**	0.310	0.352	0.116	0.188
Age (y)	71.6 ± 7.1	71.7 ± 6.1	0.470	0.703	NA	NA	NA	NA	NA	NA
Education (y)	15.9 ± 2.7	16.2 ± 2.5	1.558	0.203	NA	NA	NA	NA	NA	NA
CDR-RS	1.2 ± 0.7	2.8 ± 1.0	150.878	**<0.001**	**<0.001**	**<0.001**	**<0.001**	**<0.001**	**0.012**	**<0.001**
MMSE	27.9 ± 1.7	27.0 ± 1.6	55.520	**<0.001**	**0.129**	**0.012**	0.667	**<0.001**	**<0.001**	**<0.001**
MOCA	23.1 ± 3.2	22.6 ± 2.5	41.567	**<0.001**	**0.038**	0.062	1.000	**<0.001**	**<0.001**	**<0.001**
LM	7.2 ± 3.0	6.5 ± 3.0	87.650	**<0.001**	**<0.001**	**<0.001**	1.000	**<0.001**	**<0.001**	**<0.001**
ADAS11	8.7 ± 3.5	12.2 ± 4.3	72.559	**<0.001**	0.084	**0.001**	0.114	**<0.001**	**<0.001**	**<0.001**
ADAS13	14.0 ± 5.2	19.1 ± 6.2	86.011	**<0.001**	**0.013**	**<0.001**	**0.046**	**<0.001**	**<0.001**	**<0.001**
FAQ	2.1 ± 3.4	8.0 ± 3.1	84.147	**<0.001**	0.157	**<0.001**	**<0.001**	**<0.001**	**<0.001**	**<0.001**
AF	18.7 ± 4.8	17.8 ± 4.5	17.733	**<0.001**	0.295	0.235	1.000	**<0.001**	**0.004**	**<0.001**
BNT	27.1 ± 3.1	25.8 ± 4.9	13.471	**<0.001**	0.740	0.229	1.000	**<0.001**	**0.041**	**<0.001**
TMT-A	37.7 ± 14.9	44.0 ± 18.0	25.197	**<0.001**	1.000	0.587	0.975	**<0.001**	**<0.001**	**<0.001**
TMT-B	105.5 ± 60.4	144.4 ± 85.5	34.944	**<0.001**	1.000	**0.017**	0.080	**<0.001**	**<0.001**	**<0.001**
LDEL[#,a]	9.4 ± 2.7	8.4 ± 3.7	91.511	**<0.001**	**<0.001**	**<0.001**	1.000	**<0.001**	**<0.001**	**<0.001**
LIMM[#,a]	7.2 ± 3.0	6.5 ± 3.0	105.492	**<0.001**	**<0.001**	**<0.001**	1.000	**<0.001**	**<0.001**	**<0.001**
AVDELT[#,a]	35.9 ± 9.6	30.2 ± 4.5	38.838	**<0.001**	**<0.001**	**<0.001**	0.226	**<0.001**	0.057	**<0.001**
AVDEL30[#,a]	4.5 ± 3.7	1.5 ± 1.9	28.687	**<0.001**	**0.001**	**<0.001**	**0.011**	**<0.001**	1.000	**<0.001**
RAVLT[#,a]	11.0 ± 3.0	9.7 ± 2.3	35.416	**<0.001**	0.874	**0.002**	**0.005**	**<0.001**	**0.001**	**<0.001**
APOE ε4	37%	62%	15.428	**0.001**	0.415	0.082	0.274	**0.004**	0.622	**0.001**
Aβ (pg/mL)[##]	1246 ± 601	727 ± 357	8.976	**<0.001**	1.000	**0.003**	**0.023**	**0.003**	1.000	**0.002**
tau (pg/mL)[##]	273 ± 119	389 ± 160	7.757	**<0.001**	1.000	**0.003**	**0.017**	**0.015**	1.000	**0.002**
p-Tau (pg/mL)[##]	25.4 ± 12.5	39 ± 19	8.294	**<0.001**	1.000	**0.001**	**0.004**	**0.017**	1.000	**0.003**
t-Tau/Aβ[##]	0.29 ± 0.24	0.65 ± 0.47	13.494	**<0.001**	1.000	**<0.001**	**0.001**	**0.001**	1.000	**<0.001**
p-Tau/Aβ[##]	0.03 ± 0.02	0.07 ± 0.05	9.843	**<0.001**	1.000	**0.001**	**0.003**	**0.002**	1.000	**0.004**
L-HP/eTIV[a,b]	2.47 ± 0.44	2.28 ± 0.42	15.710	**<0.001**	0.449	0.062	0.961	**<0.001**	0.056	**<0.001**
R-HP/eTIV[a,b]	2.56 ± 0.46	2.23 ± 0.53	14.620	**<0.001**	0.940	**0.008**	0.110	**<0.001**	0.679	**<0.001**
eTIV (mm^3)[c]	1.51 ± 0.21	1.56 ± 0.23	0.442	0.723	NA	NA	NA	NA	NA	NA
L-EC (mm)	3.31 ± 0.48	3.21 ± 0.63	12.225	**<0.001**	0.601	0.463	1.000	**<0.001**	0.058	**<0.001**
R-EC (mm)	3.42 ± 0.41	3.04 ± 0.63	10.729	**<0.001**	1.000	**0.014**	**0.039**	**<0.001**	1.000	**<0.001**

Values are expressed as the mean ± standard deviation (SD). Bold values are statistically significant.
Key: APOE, apolipoprotein E; ANOVA, analysis of variance; AD, Alzheimer's disease; HC, healthy control; MCI, mild cognitive impairment; c-MCI, patients with MCI who convert to AD; nc-MCI, MCI patients who did not convert to AD; ADAS, AD Assessment Scale; AF, Animal Fluency; AVDEL30, Rey Auditory Verbal Learning Test-Delayed 30-Minute Delay Total; AVDELT, Rey Auditory Verbal Learning Test-Delayed Recognition Score; Aβ1-42, amyloid β1–42; BNT, Boston Naming Test; CDR-RS, Clinical Dementia Rating Scale; EC, entorhinal cortex; eTIV, estimated total intracranial volume; FAQ, Functional Activities Questionnaire; LDEL, Logical Memory-Delayed Recall Total Number of Story Units Recalled; LIMM, Logical Memory-Immediate Recall Total Number of Story Units Recalled; MMSE, Mini-Mental State Examination; MoCA, Montreal Cognitive Assessment; p-Tau181, tau phosphorylated at threonine 181; RAVLT, Rey Auditory Verbal Learning Test Immediate; TMT, Trail Making Test.
[#]Data on episodic memory test was not available for 1 nc-MCI patients. [##]Data on CSF biomarkers were available for 46 nc-MCI patients and 13 c-MCI patients.
[a] Right (R) and left (L) hippocampus (HP) volumes are normalized for estimated total intracranial volume.
[b] Values × 10^{-3}.
[c] Values × 10^{6}.
[d] I model: comparison between HC, nc-MCI, c-MCI, and AD.

system, and the striatum (Fig. 3D). On the other hand, compared with MCI^{AD+} patients, patients with AD showed hippocampal hypoconnectivity with core regions of the DMN/PMN and SN (posterior insula) as well as with the hypothalamus, the thalamus, the limbic system, and the striatum (Fig. 3E).

Finally, we assessed the FC changes in the nc-MCI set taking into account their load of AD-related pathology. Compared to HCs, nc-MCI^{AD-} individuals showed hippocampal hyperconnectivity with regions of the DMN and the cerebellum (Supplementary Fig. 5A). On the other hand, when compared to HCs, nc-MCI^{AD+} did not display hippocampal hyperconnectivity with DMN-related areas but showed the presence of small-size clusters of mixed patterns of hyperconnectivity and hypoconnectivity occurring between the hippocampus and the cerebellum. This set also showed hypoconnectivity of the hippocampus with the amygdala and the striatum (Supplementary Fig. 5B). Compared to nc-MCI^{AD+}, nc-MCI^{AD-} individuals showed hyperconnectivity with the cerebellum and the striatum (Supplementary Fig. 5C).

3.4. Entorhinal cortex FC variations in subsets of patients with MCI

As with the hippocampus, we first analyzed patients with MCI categorized by their clinical follow-up. Compared to HCs, nc-MCI patients showed hyper-connectivity with cerebellar areas that are part of the DMN, the FPN, the SN/CON, and the limbic system (Fig. 4A). Conversely, compared to HCs (Fig. 4B) or nc-MCI patients (Fig. 4C), c-MCI patients showed reduced connectivity with the lateral-occipital cortex, the cortical and cerebellar regions that are part of the FPN and DAN, the cerebellar regions of the SN/CON and the limbic system as well as the brainstem, the striatum, and the thalamus. Compared to nc-MCI patients, patients with AD showed diffuse patterns of entorhinal hypoconnectivity with the cerebellum, the cortical regions that are mainly involved in the SN/CON and ventral attention network as well as the thalamus, the striatum, and the brainstem (Fig. 5A). In contrast, compared to c-MCI individuals, AD patients did not show differences in hippocampal or entorhinal FC. When compared to HC patients, patients with AD displayed hypoconnectivity of the entorhinal cortex with regions of the SN/CON, the cerebellum, the brainstem, the thalamus, the striatum, and the limbic system (Fig. 5B).

In the second analysis, we evaluated the patients with MCI subdivided by their loads of AD-related pathology. In this second set, we found, that compared to HCs, MCI^{AD-} individuals showed hyperconnectivity of the entorhinal cortex with the cerebellar regions that are part of the DMN and sensorimotor network as well as with the brainstem and the striatum (Fig. 6A). In contrast, MCI^{AD+} showed hypoconnectivity with the lateral-occipital area, the striatum, and the limbic system as well as hyperconnectivity with the

Table 2
Demographic, neuropsychological, and clinical features—II model

Variable	MCI^{AD-} (N = 22, 50% male)	MCI^{AD+} (N = 37, 64% male)	ANOVA[d]		Post-hoc				
			F or μ2	*p*-value	HC vs. MCI^{AD-}	HC vs. MCI^{AD+}	MCI^{AD-} vs. MCI^{AD+}	MCI^{AD-} vs. AD	MCI^{AD+} vs. AD
Age (y)	72 ± 5.8	71.5 ± 8	1.023	0.385	NA	NA	NA	NA	NA
Education (y)	16.2 ± 2.5	15.5 ± 2.7	1.523	0.212	0.726	1.000	0.378	1.000	1.000
CDR-RS	1.9 ± 1.1	1.1 ± 0.8	131.4	**<0.001**	**<0.001**	**<0.001**	**0.020**	**<0.001**	**<0.001**
MMSE	27.4 ± 1.8	28.3 ± 1.7	66.3	**<0.001**	1.000	**0.002**	0.375	**<0.001**	**<0.001**
MOCA	23 ± 3.1	23.5 ± 2.8	50.1	**<0.001**	0.084	**0.004**	1.000	**<0.001**	**<0.001**
LM	6.7 ± 3	7.7 ± 2.6	109.8	**<0.001**	**<0.001**	**<0.001**	1.000	**<0.001**	**<0.001**
ADAS11	10.2 ± 4.4	8.3 ± 3.3	73.2	**<0.001**	0.462	**0.002**	0.933	**<0.001**	**<0.001**
ADAS13	16 ± 6.3	13.1 ± 5.3	85.8	**<0.001**	0.213	**<0.001**	0.534	**<0.001**	**<0.001**
FAQ	4.3 ± 4.7	2 ± 2.9	76.0	**<0.001**	0.603	**<0.001**	**<0.001**	0.331	0.331
AF	18.6 ± 4.6	18.9 ± 5	15.2	**<0.001**	0.911	0.340	0.340	1.000	1.000
BNT	26.5 ± 3.9	27.4 ± 2.1	14.9	**<0.001**	1.000	0.119	1.000	**<0.001**	**<0.001**
TMT-A	37 ± 13.7	38.9 ± 16.6	21.9	**<0.001**	1.000	1.000	1.000	**<0.001**	**<0.001**
TMT-B	111.4 ± 60.9	100.4 ± 55.9	31.9	**<0.001**	1.000	0.633	1.000	**<0.001**	**<0.001**
LDEL	8.8 ± 3.2	9.8 ± 2.6	87.9	**<0.001**	**<0.001**	**<0.001**	1.000	**<0.001**	**<0.001**
LIMM	6.7 ± 3	7.7 ± 2.6	109.8	**<0.001**	**<0.001**	**<0.001**	1.000	**<0.001**	**<0.001**
AVDELT	33.8 ± 7.9	35.3 ± 10.3	36.2	**<0.001**	**<0.001**	**<0.001**	1.000	**<0.001**	**<0.001**
AVDEL30	3.4 ± 3.5	4.3 ± 3.7	24.6	**<0.001**	**0.010**	**<0.001**	1.000	**<0.001**	**0.002**
RAVLT	10.2 ± 3.1	11.5 ± 2.5	36.0	**<0.001**	0.265	**<0.001**	0.490	**<0.001**	**<0.001**
L-HP/eTIV[a,b]	2.25 ± 0.43	2.23 ± 0.37	14.8	**<0.001**	1.000	**0.026**	0.203	**0.004**	**1.000**
R-HP/eTIV[a,b]	2.64 ± 0.44	2.24 ± 0.43	11.7	**<0.001**	1.000	**0.019**	0.087	**<0.001**	0.075
eTIV (mm^3)[c]	1.49 ± 0.18	1.55 ± 0.21	0.69	0.560	NA	NA	NA	NA	NA
L-EC (mm)	3.36 ± 0.52	3.20 ± 0.48	12.1	**<0.001**	1.000	0.087	1.000	**<0.001**	**0.004**
R-EC (mm)	3.48 ± 0.42	3.24 ± 0.51	9.0	**<0.001**	1.000	0.173	0.310	**<0.001**	0.060

Values are expressed as the mean ± standard deviation (SD). Bold values are statistically significant.
Note: the comparison between HC and AD is also reported in Table 2.
Key: APOE, apolipoprotein E; ANOVA, analysis of variance; AD, Alzheimer's disease; HC, healthy control; MCI, mild cognitive impairment; MCI^{AD-}, patients with MCI who did not show the presence of AD-related alterations in the cerebrospinal fluid; MCI^{AD+}, patients with MCI who showed the presence of AD-related alterations in the cerebrospinal fluid; ADAS, AD Assessment Scale; AF, Animal Fluency; AVDEL30, Rey Auditory Verbal Learning Test-Delayed 30-Minute Delay Total; AVDELT, Rey Auditory Verbal Learning Test-Delayed Recognition Score; BNT, Boston Naming Test; CDR-RS, Clinical Dementia Rating Scale; EC, entorhinal cortex; eTIV, estimated total intracranial volume; FAQ, Functional Activities Questionnaire; LDEL, Logical Memory-Delayed Recall Total Number of Story Units Recalled; LIMM, Logical Memory-Immediate Recall Total Number of Story Units Recalled; MMSE, Mini-Mental state examination; MoCA, Montreal Cognitive Assessment; RAVLT, Rey Auditory Verbal Learning Test Immediate; TMT, Trail Making Test.
[a] Right (R) and left (L) hippocampus (HP) volumes are normalized for the estimated total intracranial volume.
[b] Values × 10^{-3}.
[c] Values × 10^{6}.
[d] II model: comparison between HC, MCI^{AD-}, MCI^{AD+}, and AD.

hypothalamus. We also found a mixed pattern of hyperconnectivity and hypoconnectivity occurring between the entorhinal cortex and selected cerebellar regions (Fig. 6B). The direct comparison between the two MCI subsets revealed that MCI^{AD+} patients show entorhinal hypo-connectivity with the sensorimotor cortex, associative motor areas, DMN-related cerebellar areas and the hypothalamus and the brainstem (Fig. 6C). Compared to MCI^{AD-} patients, patients with AD showed patterns of hippocampal hypoconnectivity with the cerebellum, SN-related cortical areas, and the sensorimotor network as well as the brainstem, the hypothalamus, the limbic system, the striatum, and the thalamus (Fig. 6D). Compared to MCI^{AD+} individuals, patients with AD showed hippocampal hypo-connectivity with FPN- and SN-related cerebellar areas, the sensorimotor network, the brainstem, the striatum, and thalamus (Fig. 6E).

Table 3
Longitudinal variations of the clinical and neuropsychological test scores of the MCI subsets

Variable	nc-MCI	c-MCI
MMSE	0.36 ± 2.59	2.75 ± 4.25
MoCA[a]	−0.28 ± 2.87	4.17 ± 4.06
AF[a]	0.56 ± 4.28	6.00 ± 4.26
BNT[a]	−0.46 ± 1.92	2.25 ± 2.99
TMT-A	−0.57 ± 11.78	11.23 ± 24.06
TMT-B	1.70 ± 52.14	77.46 ± 84.86
LDEL[a]	−0.32 ± 3.26	3.50 ± 2.43
LIMM[a]	−0.44 ± 4.05	3.42 ± 3.06
AVDELT[a]	0.22 ± 6.93	5.83 ± 9.77
AVDEL30[a]	0.71 ± 3.10	1.25 ± 1.96
RAVLT[a]	0.71 ± 3.34	0.42 ± 3.06

Values are expressed as the mean ± standard deviation (SD).
Key: MCI, mild cognitive impairment; c-MCI, patients with MCI who convert to AD; nc-MCI, MCI patients who did not convert to AD; MMSE, Mini-Mental state examination; MoCA, Montreal Cognitive Assessment; AF, Animal Fluency; BNT, Boston Naming Test; AVDELT, Rey Auditory Verbal Learning Test-Delayed Recognition Score; AVDEL30, Rey Auditory Verbal Learning Test Delayed 30-Minute Delay Total; LDEL, Logical Memory-Delayed Recall Total Number of Story Units Recalled; LIMM, Logical Memory-Immediate Recall; RAVLT, Rey Auditory Verbal Learning Test Immediate; TMT, Trail Making Test.
[a] Longitudinal data on episodic memory tests were available for 92% of the MCI sample.

The third analysis investigated the nc-MCI group in reference to different loads of AD-related pathology. We found that, compared to HCs (Supplementary Fig. 6A) or nc-MCI^{AD+} (Supplementary Fig. 6C), nc-MCI^{AD-} patients showed hippocampal hyperconnectivity with selected cerebellar regions. In contrast, when compared to HC patients, nc-MCI^{AD+} patients displayed small clusters of hyperconnectivity between the entorhinal cortex and selected subcortical areas (Supplementary Fig. 6B).

3.5. Relationship of rs-fMRI data with age, morphometry, CSF biomarkers, and longitudinal changes in cognition

In the MCI group, using a whole-brain correlation analysis, we found that the features of hippocampal FC were associated with altered CSF levels of p-Tau and amyloid. Increased FC, occurring between the hippocampus and DMN regions, was negatively associated with levels of p-Tau_{181} and p-Tau_{181}/$A\beta_{1-42}$ and positively associated with $A\beta_{1-42}$ levels (Supplementary Fig. 7). The strength of the hippocampal FC did

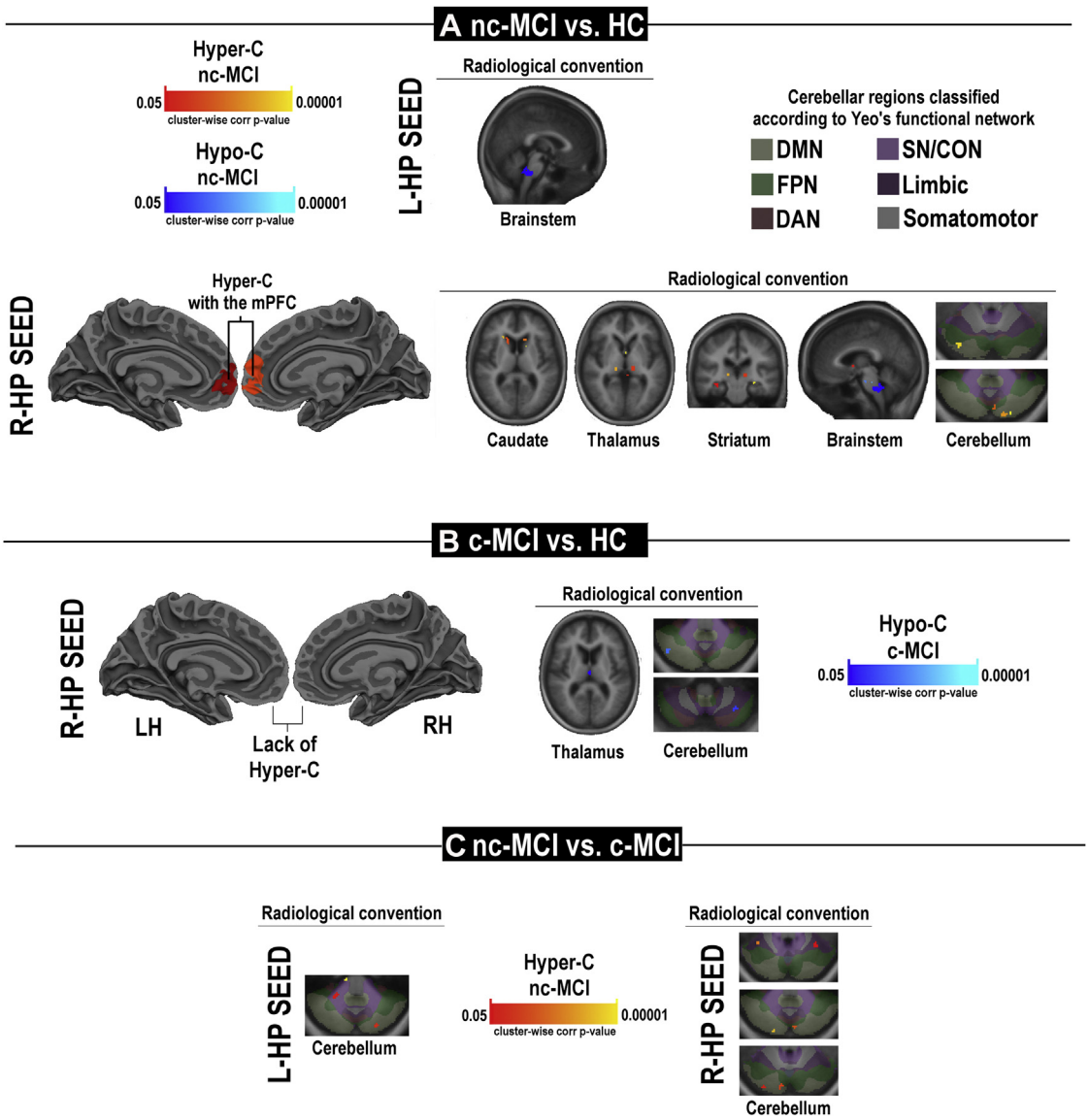

Fig. 1. Statistical maps of differences in hippocampal (HP) functional connectivity of MCI subsets. Panel A shows the comparison between nc-MCI patients and HCs; panels B and C show the comparison of c-MCI patients with HCs or nc-MCI patients, respectively. The figure depicts areas with a clusterwise probability below the corrected *p*-value of 0.05. Pseudocolor scales indicate the statistical strength of the hyperconnectivity (Hyper-C) or hypoconnectivity (Hypo-C). Clusters changing from red to yellow or from dark blue to light blue indicate increased hyper-C or hypo-C, respectively. Abbreviations: MCI, mild cognitive impairment; c-MCI, patients with MCI who convert to AD; nc-MCI, MCI patients who did not convert to AD; HC, healthy control; DAN, dorsal attention network; DMN, default-mode network; FPN, frontoparietal network; SN/CON, Salience/Cingulo-Opercular Networks; L, left; LH, left hemisphere; mPFC, medial prefrontal cortex; R, right; RH, right hemisphere. (For interpretation of the references to color in this figure legend, the reader is referred to the Web version of this article.)

not correlate with age, educational level, or alterations in the structural integrity of the hippocampus or cortex. No significant effect was found as far as the synergistic interaction of gender with respect to CSF AD-related biomarkers. In the entorhinal cortex, the strength of FC positively correlates with the structural integrity of the seed (Supplementary Fig. 8). Finally, increased hippocampal FC with the mPFC was significantly and positively associated with a smaller longitudinal decline in the Boston Naming Test and the Trail Making Test-A, two tests that evaluate naming and executive functions. The parameter also showed a trend toward significance when considering the correlation with longitudinal changes in scores of the Rey Auditory Verbal Learning Test-Delayed 30-Minute Delay Total (Tables 3 and 4). Moreover, the increase of hippocampal FC was significantly associated with smaller longitudinal variations in cognition. Conjunction maps show that these relationships are linked to variations of episodic memory (Rey Auditory Verbal Learning Test) and executive functions (Trail Making Test-B) (Fig. 7). These findings indicate that the increased hippocampal FC can help to maintain performances in subsets of cognitive domains.

4. Discussion

In the present study, we investigated patterns of hippocampal and entorhinal FC in a cohort of HCs, patients with MCI, and patients with AD. The rs-fMRI data were also evaluated in relation to the clinical progression and degrees of AD pathology of patients with MCI. Overall, the analysis indicates that patients with AD show a parallel process of hypoconnectivity that is localized in the

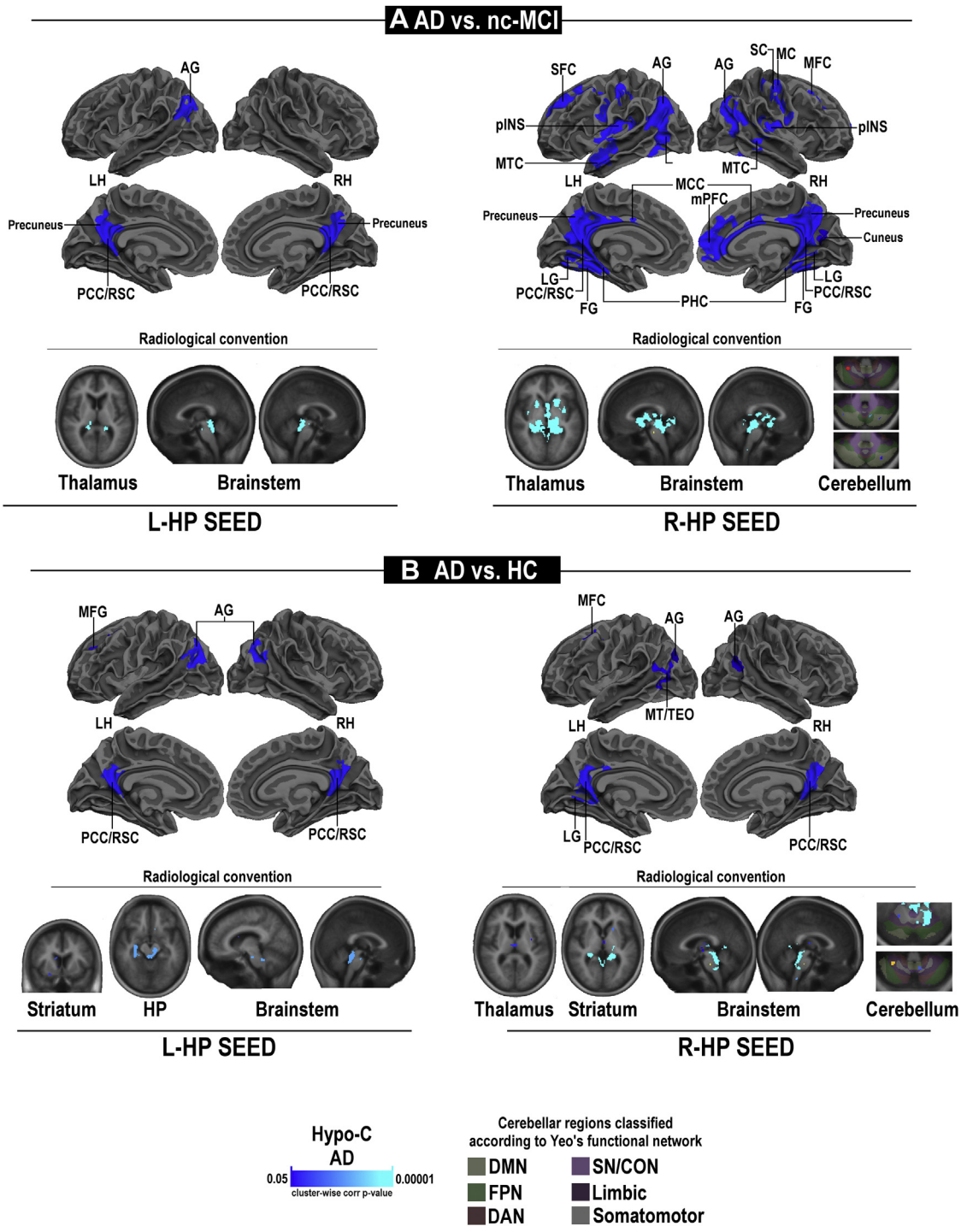

Fig. 2. Statistical maps of differences in hippocampal (HP) functional connectivity of patients with AD. Significant hypoconnectivity is observed in patients with AD when compared to nc-MCI patients (panel A) or HCs (panel B). The figure depicts areas with a clusterwise probability below the corrected *p*-value of 0.05. Pseudocolor scales, with clusters changing from dark blue to light blue, indicate the statistical strength of the hypoconnectivity (Hypo-C). Abbreviations: c-MCI, patients with MCI who convert to AD; nc-MCI, MCI patients who did not convert to AD; HC, healthy control; AG, angular gyrus; DAN, dorsal attention network; DMN, default-mode network; FG, fusiform gyrus; FPN, frontoparietal network; IPL, interior parietal lobe; L, left; LH, left hemisphere; LG, lingual gyrus; MC, motor cortex; MCC, middle cingulate cortex; MFG/MFC, middle frontal gyrus/cortex; MT, middle temporal area; MTC, middle temporal cortex; pINS, posterior insula; SMA, supplementary motor area; mPFC, medial prefrontal cortex; PCC/RSC, posterior cingulate cortex/retrosplenial cortex; PHC, parahippocampal cortex; R, right; RH, right hemisphere; SC, sensory cortex; SFC, superior frontal cortex; SN/CON, Salience/Cingulo-Opercular Networks; TEO, posterior inferior temporal cortex. (For interpretation of the references to color in this figure legend, the reader is referred to the Web version of this article.)

hippocampus and entorhinal cortex. The analysis of the MCI subsets shows that c-MCI and MCI^{AD+} patients are characterized by hypoconnectivity of the entorhinal cortex and hippocampus while nc-MCI and MCI^{AD-} patients exhibit hyperconnectivity of the two regions.

4.1. Patterns of functional connectivity, cognitive status, and structural damage of patients with AD

Our patients with AD were characterized by the collapse of hippocampal and entorhinal connectivity, the decline in memory and

executive skills, and the presence of marked signs of cortical atrophy and subcortical atrophy. These findings confirm the notion that macrostructural damage severely impairs global communication efficiency, prevents the adaptive functional reorganization of the brain networks, ultimately setting the stage for the disease progression (Hillary and Grafman, 2017). Of note, we observed hypoconnectivity in the angular gyrus and retrosplenial/posterior cingulate cortex, two areas that are strictly involved in memory retrieval and intimately connected to the hippocampus and entorhinal cortex (Eichenbaum, 2017; Sestieri et al., 2017). It is therefore conceivable that, in patients with AD, the reduced connectivity of the hippocampus and entorhinal cortex represents a functional correlate of the defective episodic memory retrieval that is found in the disease.

4.2. Patterns of functional connectivity, cognitive status, and structural features of nc-MCI and MCI^{AD-} patients

Our study shows that nc-MCI and MCI^{AD-} individuals exhibit hippocampal and entorhinal hyperconnectivity as well as the relative preservation of cognitive functions and brain structures.

The hippocampal hyperactivity exhibited by patients with MCI is controversial in value. Although some authors have proposed that the process plays a compensatory role and helps to maintain cognitive performances (Bondi et al., 2005; Dai et al., 2009; Dickerson and sperling, 2008; Huijbers et al., 2015; Kircher et al., 2007; Mormino et al., 2011; Oh and Jagust, 2013; Putcha et al., 2011; Schultz et al., 2017; Sperling et al., 2009), others have considered the phenomenon disadvantageous and set to promote cognitive impairment (Das et al., 2013; Pasquini et al., 2015).

Furthermore, previous studies have indicated that patients with MCI show hyperconnectivity or hyperactivity that is regionally restricted within the medial temporal lobe (MTL) while reduced connectivity occurs between MTL and other network nodes, including the DMN. These intra-MTL effects have been confirmed by Arterial Spin Labeling studies (Alsop et al., 2008, 2010), task fMRI (Yassa et al., 2010b), and rs-fMRI (Das et al., 2013; Pasquini et al., 2015). We have performed the MTL analysis and found that, compared to HC or nc-MCI groups, the mean values of intra-MTL connectivity are higher in the AD or c-MCI sets. However, these FC differences did not reach statistical significance (data not shown), thereby suggesting differences between our and the other (Das et al., 2013; Pasquini et al., 2015) data sets.

Our results, indicating the presence of enhanced FC between the hippocampus, thalamus, striatum, and the mPFC support the "compensatory hypothesis" for the hyperconnectivity that we have detected. The thalamus is a structural and functional hub for the communication occurring between the hippocampus and mPFC, thereby favoring strategic cognitive functions, including memory consolidation (Eichenbaum, 2017; Ferraris et al., 2018). The striatum, along with the PFC, is also implicated in the modulation of memory retrieval (Scimeca and Badre, 2012). The mPFC is part of an integrated system, the DMN, that sustains the global communication and metastability of the brain (Hellyer et al., 2014) and, ultimately, affects a wide range of high-order cognitive functions and the resilience against neurodegenerative processes (Hillary and Grafman, 2017). The hippocampal hyperconnectivity with the mPFC is in line with different proposed modelizations of brain aging (i.e., HERA, HAROLD, PASA, CRUNCH, STAC, GOLDEN Aging) that postulate that the increased engagement of the prefrontal brain regions is set to compensate the functional decline occurring in posterior regions of the brain (Cabeza et al., 1997; Davis et al., 2008; Fabiani, 2012; Park and Reuter-Lorenz, 2009; Reuter-Lorenz and Park, 2014; Schneider-Garces et al., 2010; Tulving et al., 1994). The compensatory hypothesis fits with evidence indicating that the mPFC and the hippocampus are tightly interconnected by bidirectional projections that are structurally and functionally integrated. The oscillatory synchronic activity between these two regions supports the organization and processing of the episodic memory (Eichenbaum, 2017). The mPFC is strategic for memory as the area receives information on contextual cues from the anterior hippocampus and, in turns, indirectly sends the information—via the thalamus and perirhinal/entorhinal cortices—to the posterior hippocampus (Supplementary Fig. 9). In this context, the hippocampus acts as a key region that is set to control memory organization and encoding, whereas the mPFC is implicated in the retrieval of context-appropriate memory engrams, the suppression of distractors or the interference, and switching or selection of episodic memories according to contextual rules (Eichenbaum, 2017). Furthermore, the presence of altered connectivity between the mPFC and the hippocampus impairs the object-place and temporal-order memory and leads to severe impairment of conditional visual discrimination as well as to learning and memory deficits related to defective suppression of irrelevant memory engrams (Barker et al., 2007; Eichenbaum, 2017). In summary, the enhanced FC between the hippocampus and the mPFC that we observed in the nc-MCI group is likely to result in positive cognitive outputs.

Our findings also unravel a functional connection between the hippocampus and the cerebellum. The comparison with HCs or within MCI subsets revealed that nc-MCI and MCI^{AD-} individuals show hippocampal hyperconnectivity with cerebellar areas that are functionally associated with the DMN. The interplay between these regions—through circuits that involve the entorhinal cortex, the cerebellum-thalamo-cortical, and cortica-ponto-cerebellar pathways—is strategic for the modulation of cognitively relevant prefrontal and parietal activities (Yu and Krook-Magnuson, 2015). The involvement of the cerebellum is intriguing as recent evidence indicates that the region acts as a critical hub for the control of a wide range of cognitive processes encompassing language, visual-spatial, executive, and working memory processes (Stoodley, 2012). In that regard, we found that the hippocampal hyperconnectivity of the nc-MCI or MCI^{AD-} subsets was associated with the preservation of cognition, and mnestic and executive functions, in particular, thereby suggesting that the cerebellum can be strategically involved in maintaining the cognitive reserve (Fig. 7).

From a theoretical standpoint, the increased FC that we observed in nc-MCI patients may help to cope with and counteract the undergoing neurodegenerative process and related cognitive impairment. These speculative considerations are inferred from a model that is pseudolongitudinal as the data set offers information on the clinical progression but not on the related longitudinal FC changes. However, the overlap of findings that we observed between nc-MCI patients who are also MCI^{AD-} lend support to the idea that the hippocampal hyperconnectivity of MCI individuals—when the AD-related pathology is not present or at subthreshold levels—serves as a valuable adaptive strategy to maintain cognitive functions. Our findings also lend support to the possibility of a previously described "inverse U-shaped" model and proposes that divergent patterns of hippocampal FC can be used as functional biomarker to identify the presence or absence of dynamic processes that drive MCI patients to AD (Dickerson and Sperling, 2008; Schultz et al., 2017; Sperling et al., 2010, 2014).

4.3. Patterns of functional connectivity, cognitive status, and structural alterations in c-MCI and MCI^{AD+} patients

c-MCI and MCI^{AD+} patients did not show signs of hippocampal hyperconnectivity with the mPFC, DMN-related areas or the

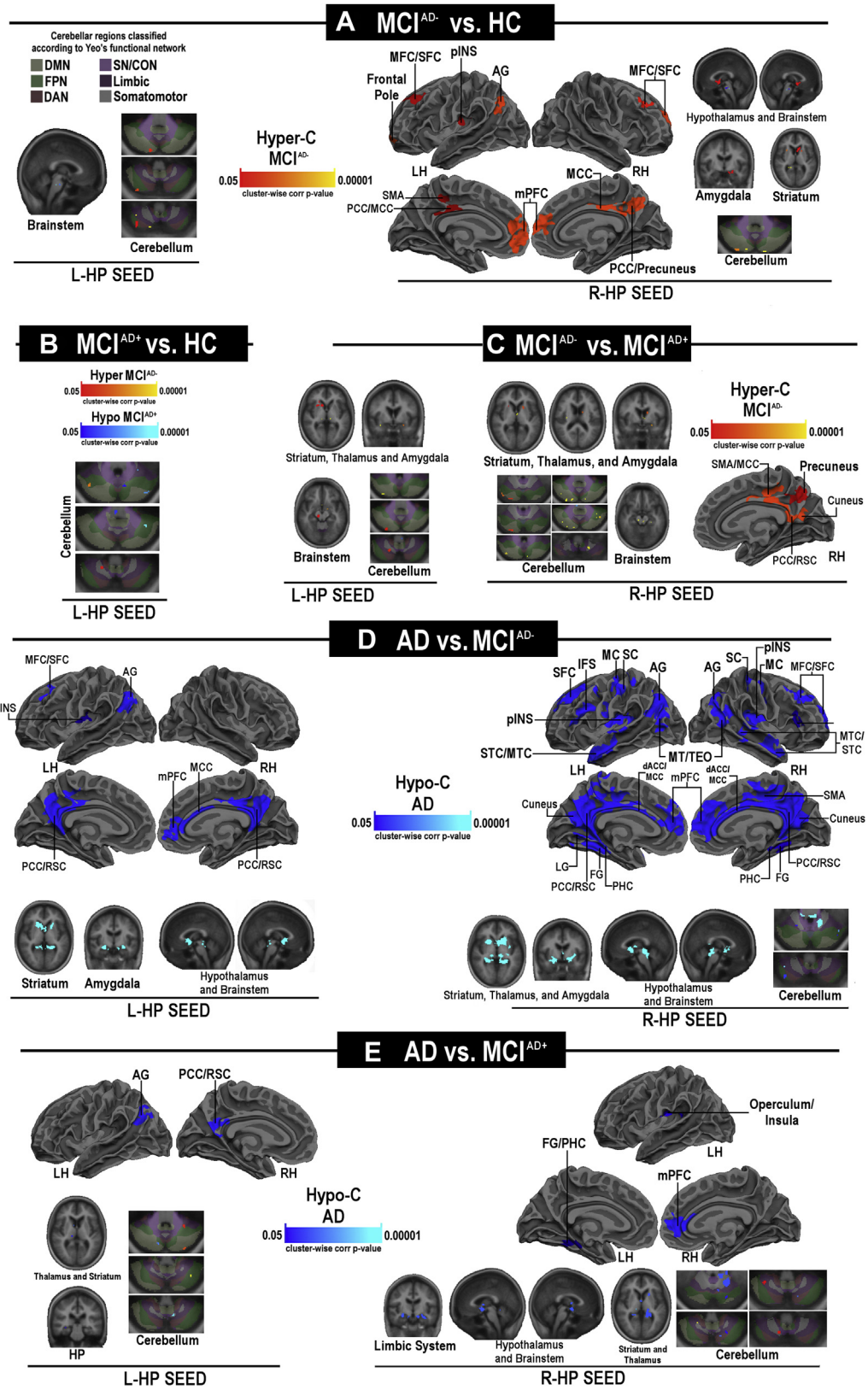

Fig. 3. Statistical maps of differences in hippocampal (HP) functional connectivity of MCI subtypes categorized by the p-Tau/Aβ ratio. Panels A and B show the comparison between HC and MCI^{AD-} or MCI^{AD+} individuals, respectively; panel C shows the comparison between the two MCI subsets. Panels D and E show connectivity changes in patients with AD when compared to MCI^{AD-} or MCI^{AD+} patients, respectively. The figure depicts areas with a clusterwise probability below the corrected *p*-value of 0.05. Clusters changing from red to yellow or from dark blue to light blue indicate increased hyper-C or hypo-C, respectively; Abbreviations: MCI, mild cognitive impairment; MCI^{AD-}, patients with MCI who did not show the presence of AD-related alterations in the cerebrospinal fluid; MCI^{AD+}, patients with MCI who showed the presence of AD-related alterations in the cerebrospinal fluid; HC, healthy controls; AG, angular gyrus; dACC, dorsal anterior cingulate cortex; DAN, dorsal attention network; DMN, default-mode network; FG, fusiform gyrus; FPN, frontoparietal network; L, left; LH, left hemisphere; LG, lingual gyrus; IFS, inferior frontal sulcus; MC, motor cortex; MCC, middle cingulate cortex; MFG/MFC, middle frontal gyrus/cortex; MTC, middle temporal cortex; SMA, supplementary motor area; mPFC, medial prefrontal cortex; PCC/RSC, posterior cingulate cortex/retrosplenial cortex; PHC, parahippocampal cortex; pINS, posterior insula; R, right; RH, right hemisphere; SC, sensory cortex; SFC, superior frontal cortex; SN/CON, Salience/Cingulo-Opercular Networks; STC, superior temporal cortex. (For interpretation of the references to color in this figure legend, the reader is referred to the Web version of this article.)

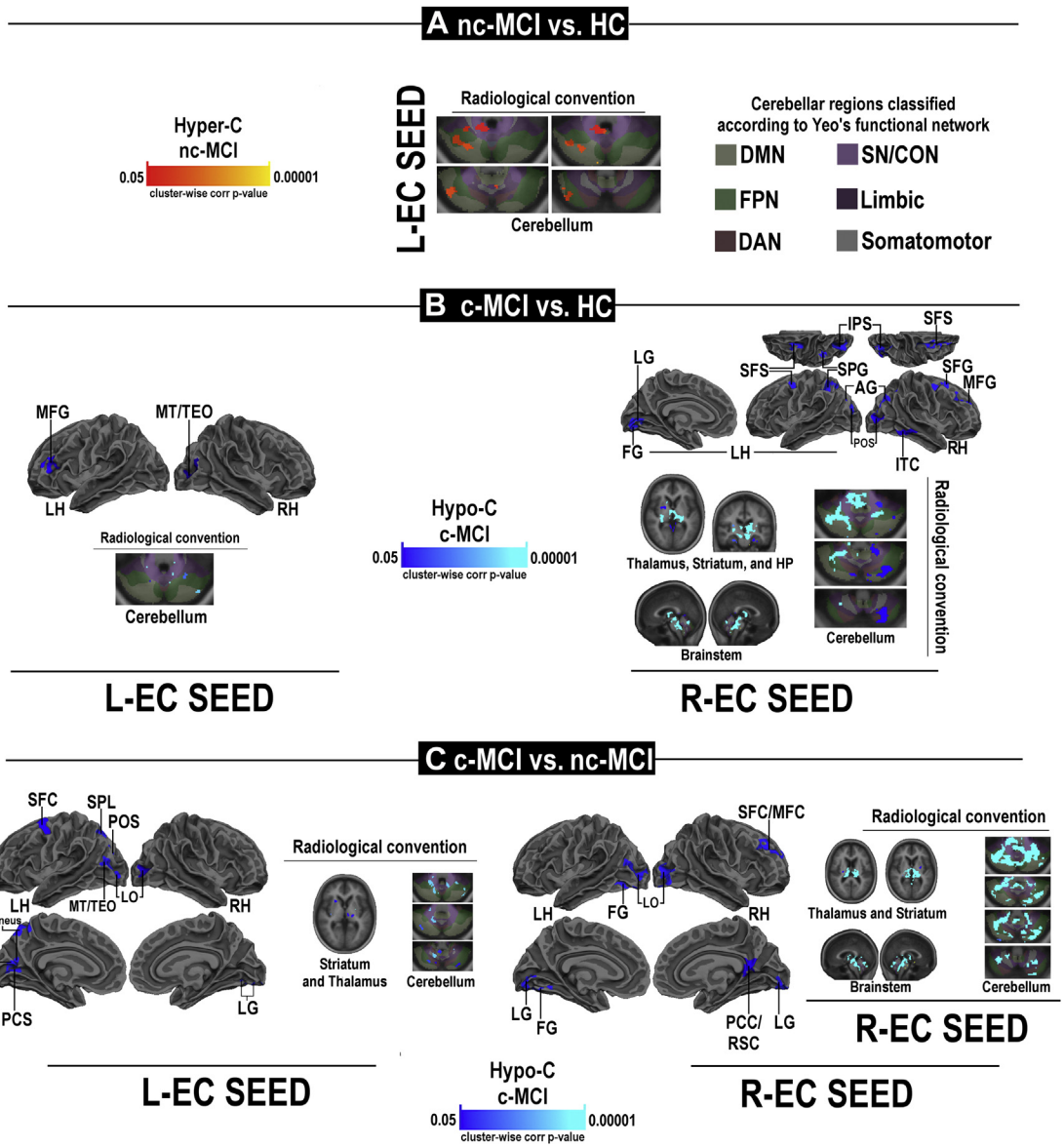

Fig. 4. Statistical maps of differences in entorhinal (EC) functional connectivity of MCI subsets. Panel A shows the comparison between nc-MCI patients and HCs; panels B and C show the comparison of c-MCI patients with HCs or nc-MCI patients, respectively. The figure depicts areas with a clusterwise probability below the corrected *p*-value of 0.05. Clusters changing from red to yellow or from dark blue to light blue indicate increased hyper-C or hypo-C, respectively. Abbreviations: MCI, mild cognitive impairment; c-MCI, patients with MCI who convert to AD; nc-MCI, MCI patients who did not convert to AD; HC, healthy control; AG, angular gyrus; DAN, dorsal attention network; DMN, default-mode network; FG, fusiform gyrus; FPN, fronto-parietal network; IPS, intraparietal sulcus; ITC, inferior temporal cortex; L, left; LG, lingual gyrus; LH, left hemisphere; LO, lateral-occipital; MFC, middle frontal cortex; MFG, middle frontal gyrus; PCC/RSC, posterior cingulate cortex/retrosplenial cortex; PCS, paracingulate sulcus; POS, parieto-occipital sulcus; R, right; RH, right hemisphere; SN/CON, Salience/Cingulo-Opercular Networks; SFC, superior frontal cortex; SFG, superior frontal gyrus; SFS, superior frontal sulcus; SPG, superior parietal gyrus; SPL, superior parietal lobe. (For interpretation of the references to color in this figure legend, the reader is referred to the Web version of this article.)

cerebellum. This lack of hyperconnectivity may result in reduced compensatory engagement of critical regions that are involved in the brain metastability and lead to more severe cognitive decline. c-MCI and MCI^{AD+} individuals also showed entorhinal hypo-connectivity with cortical and cerebellar regions that take part in the modulation of long-term memory and attentional systems. The entorhinal hypoconnectivity should be considered in relation to the role played by the superficial layers, II-III, of this region (Supplementary Fig. 9). These layers act as relay stations that carry, through the perirhinal or parahippocampal cortices, unimodal/multimodal cortical information from cortical associative areas to the hippocampus (Canto et al., 2008; Ranganath and Ritchey, 2012). Moreover, the deep layers, V-VI, of the lateral entorhinal cortex send projections from the posterior hippocampus, via the cingulum, to the parahippocampus and the cortical areas that are involved in attentional networks and the DMN/PMN bundle (Kahn et al., 2008; Lacy and Stark, 2012; Libby et al., 2012). These circuits promote the integration of spatial information and the representation of retrieved events (Preston and Eichenbaum, 2013; Vann et al., 2009). It is therefore conceivable that, in c-MCI patients, reduced FC with the DMN and associative networks represents a functional marker of underlying alterations that occur before the onset and development of AD.

In line with previous MRI studies (Apostolova et al., 2006; Dickerson and sperling, 2008; Grundman et al., 2002; Henneman et al., 2009; Jack et al., 2004), c-MCI patients show mesial

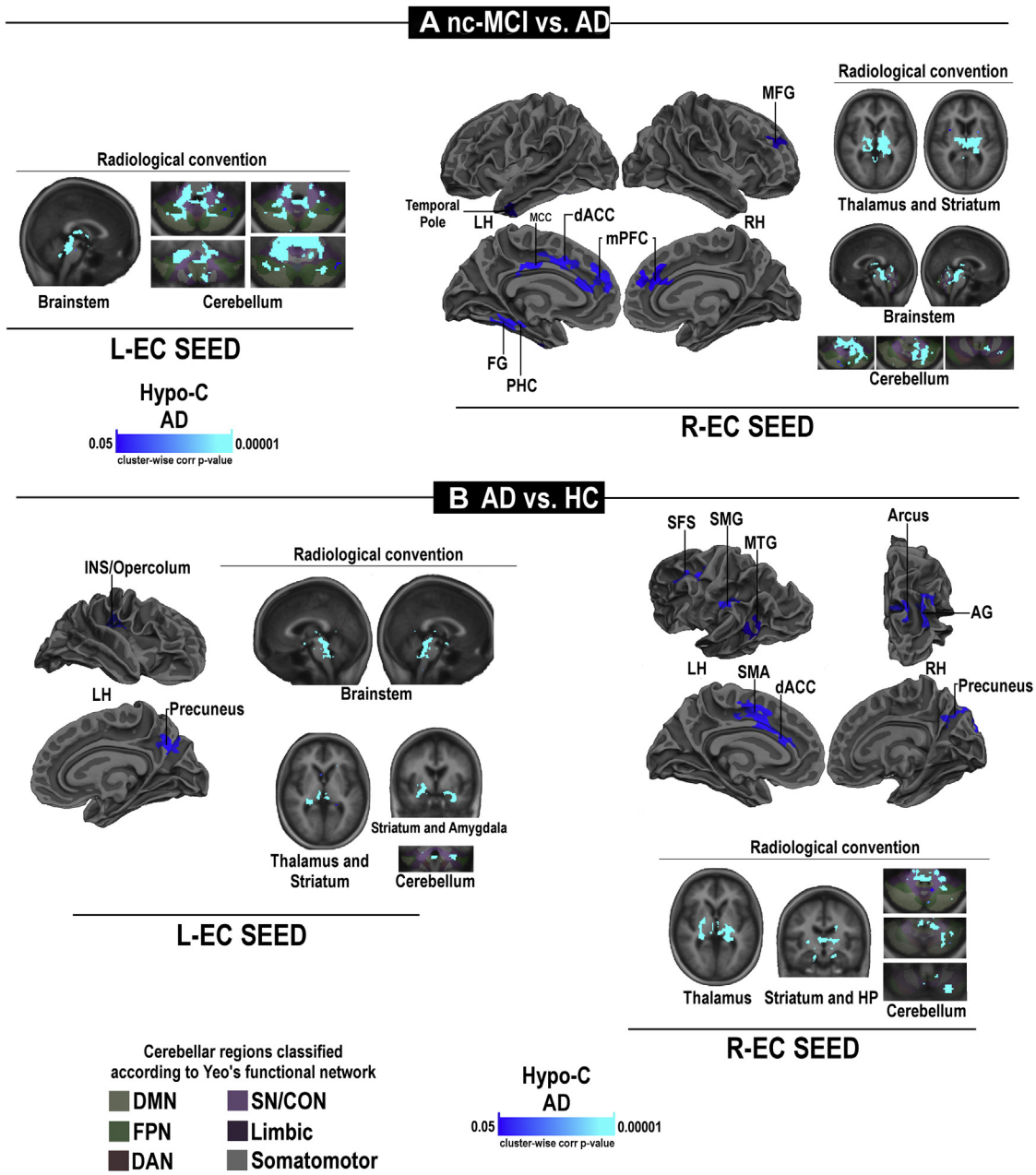

Fig. 5. Statistical maps of differences in entorhinal (EC) functional connectivity of patients with AD. Significant hypoconnectivity is observed in patients with AD when compared to nc-MCI patients (panel A), c-MCI patients (panel B), or HCs (panel C). The figure depicts areas with a clusterwise probability below the corrected *p*-value of 0.05. Pseudocolor scales, with clusters changing from dark blue to light blue, indicate the statistical strength of the hypoconnectivity (Hypo-C). Abbreviations: MCI, mild cognitive impairment; nc-MCI, MCI patients who did not convert to AD; HC, healthy control; AG, angular gyrus; dACC, dorsal anterior cingulate cortex; DAN, dorsal attention network; DMN, default-mode network; FG, fusiform gyrus; FPN, frontoparietal network; INS, insula; L, left; LH, left hemisphere; MCC, middle cingulate cortex; MFC, middle frontal cortex; mPFC, medial prefrontal cortex; MTG, middle temporal gyrus; PHC, parahippocampal cortex; R, right; RH, right hemisphere; SFS, superior frontal sulcus; SMG, supramarginal gyrus; SMA, Supplementary Motor Area; SN/CON, Salience/Cingulo-Opercular Networks. (For interpretation of the references to color in this figure legend, the reader is referred to the Web version of this article.)

temporal atrophy in the hippocampus and entorhinal cortex. Although some studies have reported the presence of cortical atrophy in patients with MCI (Tabatabaei-Jafari et al., 2015), our MCI individuals were characterized by relative preservation of the cortical thickness. In that regard, it should be underlined that these patients did not show a substantial impairment of the global cognitive functions. In addition, our study patients were highly educated individuals who likely possessed significant levels of cognitive reserve (Lo and Jagust, 2013).

Overall, these data are in agreement with neuropathological evidence indicating that the entorhinal cortex and the hippocampus are the first brain regions to display tau pathology and neurodegeneration in the course of AD (Braak et al., 1994). In line with this notion, our c-MCI patients showed decreased CSF levels of $A\beta_{1-42}$ and increased levels of t-Tau, p-Tau_{181}, t-Tau/$A\beta_{1-42}$, and p-Tau_{181}/$A\beta_{1-42}$, alterations that went along with the presence of more significant memory deficits.

The correlation between altered CSF features and the presence of mPFC-related modifications is in accordance with studies showing that decreased FC between central hubs of the DMN correlates with enhanced Aβ deposition (Buckner et al., 2005; Elman et al., 2016; Foster et al., 2018; Grothe and teipel, 2016;

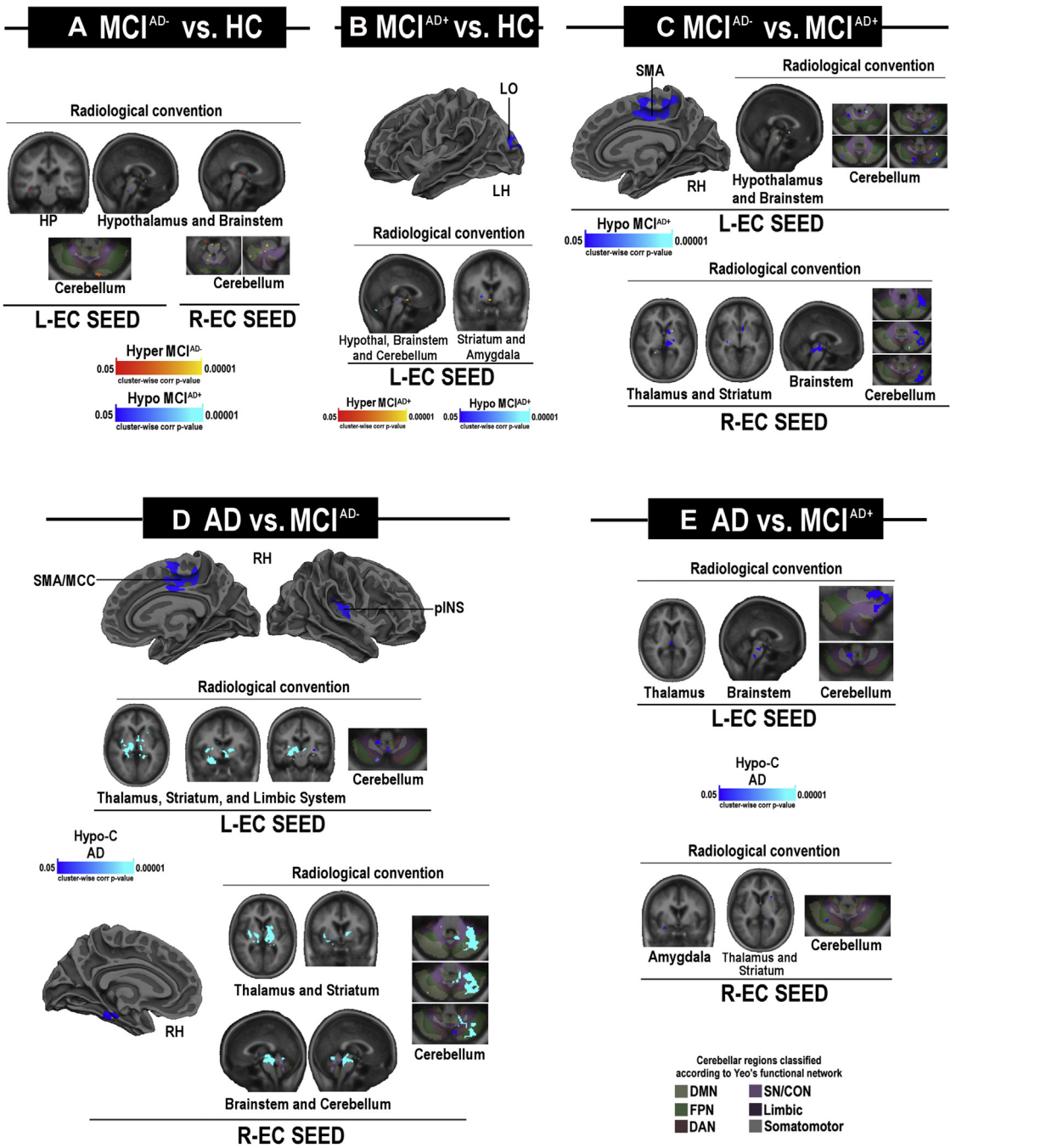

Fig. 6. Statistical maps of differences in entorhinal (EC) functional connectivity of MCI subtypes categorized by the p-Tau/Aβ ratio. Panels A and B show the comparison between HC and MCI^{AD-} or MCI^{AD+} individuals, respectively; panel C shows the comparison between the two MCI subsets. Panels D and E show the connectivity changes in patients with AD when compared to MCI^{AD-} or MCI^{AD+} patients, respectively. The figure depicts areas with a clusterwise probability below the corrected *p*-value of 0.05. Clusters changing from red to yellow or from dark blue to light blue indicate increased hyper-C or hypo-C, respectively; Abbreviations: MCI, mild cognitive impairment; MCI^{AD-}, patients with MCI who did not show the presence of AD-related alterations in the cerebrospinal fluid; MCI^{AD+}, patients with MCI who showed the presence of AD-related alterations in the cerebrospinal fluid; HC, healthy controls; DAN, dorsal attention network; DMN, default-mode network; FPN, fronto-parietal network; L, left; LH, left hemisphere; LO, lateral-occipital; MCC, middle cingulate cortex; pINS, posterior insula; SMA, supplementary motor area; R, right; RH, right hemisphere; SN/CON, Salience/Cingulo-Opercular Networks. (For interpretation of the references to color in this figure legend, the reader is referred to the Web version of this article.)

Koch et al., 2010; Mormino et al., 2011; Mutlu et al., 2017; Palmqvist et al., 2017). fMRI/PET studies have recently shown that increased levels of tau-related pathology lead to a progressive decline of the brain FC (Cope et al., 2018; Hoenig et al., 2018; Jones et al., 2016; Sepulcre et al., 2017) and reduced activation of the DMN in particular (Hoenig et al., 2018). Schultz et al (2017) have also suggested that, upon presymptomatic AD, a transient hyperconnectivity phase is followed by hypoconnectivity. The authors reported that DMN connectivity is negatively associated with global cortical deposition of amyloid and the presence of PET-related signs of tau pathology in the MTL and inferior parietal cortices. These fMRI/PET findings and our data fit with a model in which the appearance of signs of tau pathology go along with the loss of hippocampal GABAergic interneurons that may be instrumental in setting the stage for regional hyperexcitability (Levenga et al., 2013).

Table 4
Relationships between FC strength and longitudinal changes in cognition

FC strength of R-HP with	Statistics	MMSE	MOCA	AF	BNT	TMT-A	TMT-B	LDEL	LIMM	AVDELT	AVDEL30	RAVLT
L-mPFC	Corr. Coeff.	0.019	−0.201	−0.093	**−0.305***	**−0.241***	−0.087	0.075	−0.136	−0.074	−0.102	0.025
	p-value	0.885	0.116	0.472	**0.016**	**0.050**	0.482	0.562	0.293	0.570	0.433	0.849
R-mPFC	Corr. Coeff.	−0.061	**−0.217**	−0.066	**−0.267***	−0.148	−0.050	0.070	−0.082	−0.075	**−0.222**	0.059
	p-value	0.637	**0.091**	0.609	**0.036**	0.232	0.686	0.590	0.529	0.566	**0.086**	0.649

An asterisk indicates statistical significance. Bold values are statistically significant.
Key: AVDELT, Rey Auditory Verbal Learning Test-Delayed Recognition Score; AVDEL30, Rey Auditory Verbal Learning Test Delayed 30-Minute Delay Total; AF, Animal Fluency; BNT, Boston Naming Test; FC, functional connectivity; HP, hippocampus; L, left; mPFC, medial prefrontal cortex; LDEL, Logical Memory-Delayed Recall Total Number of Story Units Recalled; LIMM, Logical Memory-Immediate Recall Total Number of Story Units Recalled; MMSE, Mini-Mental State Examination; MOCA, Montreal-Cognitive Assessment; R, right; RAVLT, Rey Auditory Verbal Learning Total Number of Story Units Recalled; MMSE, Mini-Mental State Examination; MoCA, Montreal Cognitive Assessment; TMT, Trail Making Test; RAVLT, Rey Auditory Verbal Learning.

We, therefore, propose a "work in progress" model (Fig. 8) where patterns of altered hippocampal FC can serve as a proxy functional biomarker of the susceptibility to AD status of subsets of patients with MCI. The model proposes a two-stage process. In MCI^{AD-} patients, the benign, paraphysiological, occurrence of tau deposition that is restricted to the MTL (Braak et al., 1994, 2013) (Ossenkoppele et al., 2016; Scholl et al., 2016) may favor a down-regulation of GABAergic neurotransmission that sustains a compensatory and cognitively relevant enhanced glutamatergic neurotransmission and excitability. In MCI^{AD+} patients, the pathological load produced by the convergence of amyloid-dependent and -independent mechanisms may accelerate injurious tau deposition outside the MTL (Braak et al., 1994, 2013), unleash a glutamatergic overdrive, and favors the onset of pathological hyperexcitability, excitotoxicity, microstructural/macrostructural damage, atrophy, deficient hippocampal functioning, and the progression of cognitive and behavioral disorders (Frazzini et al., 2016; Gilani et al., 2014; Jones et al., 2016; Palop and Mucke, 2016; Schmitz et al., 2017; Schobel et al., 2013). This hypothesis finds some support by the combined analysis of the MCI subgroups. We find that the hyperconnectivity of nc-MCI patients is inhibited by the presence of the AD-related pathology as, of a total of 54 nc-MCI patients, the phenomenon is missing in 25 who are AD^{+} (Supplementary Fig. 2). On the other hand, in our MCI set, the presence of the AD-related pathology is not sufficient, at least in the two-year timeframe of the data set, to promote the conversion to AD. A crossed analysis (nc/c; AD+/-) shows in fact that as, of a total of 37 nc-MCI patients, 25 are also AD^{+}, a finding that is in line with the current view of AD as a multifactorial condition driven by amyloid-dependent and independent mechanisms.

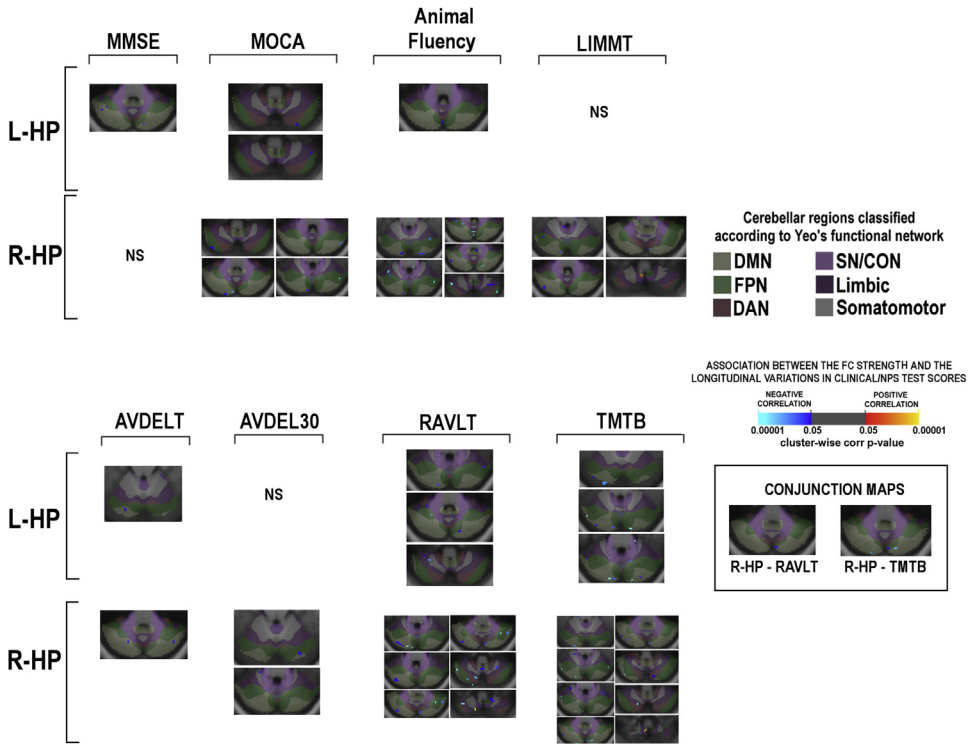

Fig. 7. Whole-cerebellum correlation analysis between hippocampal (HP) functional connectivity and longitudinal variations of neuropsychological/clinical scores. Each conjunction map shows the intersection of significant clusters that indicate correlations between FC and longitudinal variations of RAVLT and TMT-B scores and clusters expressing significant FC differences in the comparisons between nc-MCI and c-MCI. Clusters changing from red to yellow or from dark blue to light blue indicate positive or negative correlations, respectively. Images are shown in radiological convention. Note that the enhanced hippocampal FC is associated with lower longitudinal decline in cognitive domains assessed by the RAVLT and TMT-B. Abbreviations: DAN, dorsal attention network; DMN, default-mode network; FPN, fronto-parietal network; SN/CON, Salience/Cingulo-Opercular Networks; MMSE, Mini-Mental state examination; FC, functional connectivity; MoCA, Montreal Cognitive Assessment; BNT, Boston Naming Test; AVDELT, Rey Auditory Verbal Learning Test-Delayed Recognition Score; AVDEL30, Rey Auditory Verbal Learning Test Delayed 30-Minute Delay Total; LDEL, LIMMT, Logical Memory-Immediate Recall Total Number of Story Units Recalled; NS, not significant; TMT-B, Trail Making Test Part B; RAVLT, Rey Auditory Verbal Learning Test Immediate; NPS, neuropsychological. (For interpretation of the references to color in this figure legend, the reader is referred to the Web version of this article.)

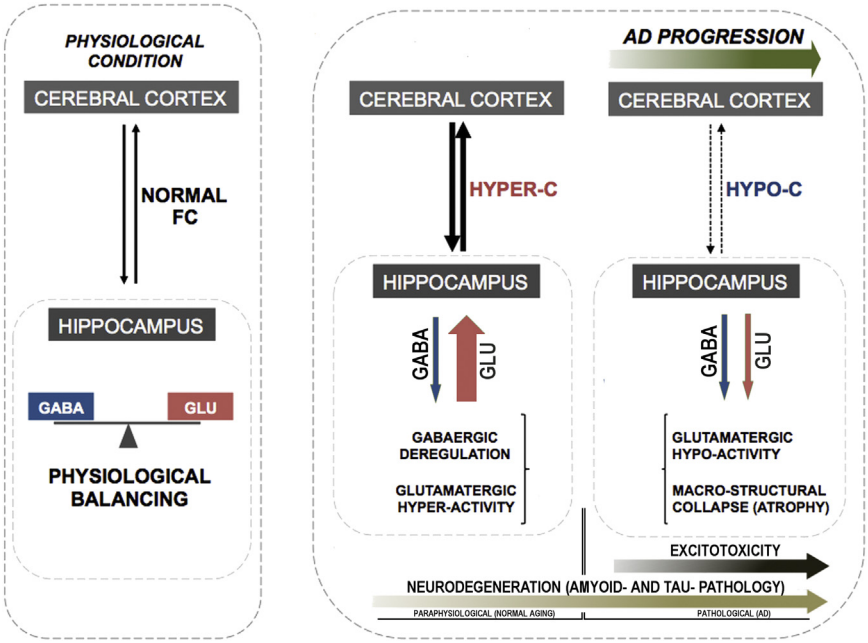

Fig. 8. Proposed model of changes in hippocampal connectivity that occur at different stages of the AD spectrum. In MCI^{AD-} patients, the paraphysiological occurrence of tau deposition, a phenomenon restricted to the MTL, may favor the downregulation of GABAergic neurotransmission that can promote compensatory, cognitively relevant, hyperexcitability. In MCI^{AD+} patients, the convergence of amyloid-dependent and -independent mechanisms may favor the transition to widespread and patent tau pathology, thereby unleashing a glutamatergic overdrive, pathological hyperexcitability, excitotoxicity, microstructural/macrostructural damage, atrophy, deficient hippocampal functioning, and the progression to cognitive and behavioral disorders. Abbreviations: AD, Alzheimer's disease; MCI, mild cognitive impairment; MCI^{AD-}, patients with MCI who did not show the presence of AD-related alterations in the cerebrospinal fluid; MCI^{AD+}, patients with MCI who showed the presence of AD-related alterations in the cerebrospinal fluid; MTL, medial temporal lobe.

Further investigations, combining proton MR spectroscopy and rs-fMRI, will be needed to test this hypothesis and understand the nature and precise timeline of the functional changes occurring in MCI individuals along with their molecular underpinnings.

5. Conclusions

The study identifies the functional correlates of alterations that occur in patients with MCI. Our study has some limitations. For instance, the neuropsychological tests used in the ADNI database are skewed toward the investigation of mnemonic domains and do not allow a detailed analysis of visuospatial and attentional domains. The data set does offer information on the longitudinal variations of the fMRI changes, an issue that should be addressed by future investigation. Finally, the model should be tested and further validated by investigating changes in functional and structural connectivity in relation to ongoing processes of amyloid and tau deposition, brain metabolism, and synaptic density as assessed by PET imaging. The study nevertheless offers a functional biomarker that can be used in selected diagnostic settings and may indicate a window of therapeutic opportunity in subsets of patients with MCI.

Acknowledgements

This work was supported by research grants from the Italian Department of Education (PRIN 2011; 2010M2JARJ_005), the Italian Department of Health (RF-2013–02358785 and NET-2011-02346784-1), and from the AIRAlzh Onlus (ANCC-COOP).

Data collection and sharing for this project were funded by the ADNI (National Institutes of Health Grant U01 AG024904). ADNI is funded by the National Institute on Aging, the National Institute of Biomedical Imaging and Bioengineering, and through generous contributions from the following: AbbVie, Alzheimer's Association; Alzheimer's Drug Discovery Foundation; Araclon Biotech; BioClinica, Inc.; Biogen; Bristol-Myers Squibb Company; CereSpir, Inc.; Cogstate; Eisai Inc.; Elan Pharmaceuticals, Inc.; Eli Lilly and Company; EuroImmun; F. Hoffmann-La Roche Ltd and its affiliated company Genentech, Inc.; Fujirebio; GE Healthcare; IXICO Ltd.; Janssen Alzheimer Immunotherapy Research & Development, LLC.; Johnson & Johnson Pharmaceutical Research & Development LLC.; Lumosity; Lundbeck; Merck & Co., Inc.; Meso Scale Diagnostics, LLC.; NeuroRx Research; Neurotrack Technologies; Novartis Pharmaceuticals Corporation; Pfizer Inc.; Piramal Imaging; Servier; Takeda Pharmaceutical Company; and Transition Therapeutics. The Canadian Institutes of Health Research is providing funds to support ADNI clinical sites in Canada. Private sector contributions are facilitated by the Foundation for the National Institutes of Health (www.fnih.org). The grantee organization is the Northern California Institute for Research and Education, and the study is coordinated by the Alzheimer's Therapeutic Research Institute at the University of Southern California. ADNI data are disseminated by the Laboratory for Neuro Imaging at the University of Southern California.

The authors are grateful to all the members of the Molecular Neurology Unit for helpful discussions and to Dr. Domenico Ciavardelli for helping with the statistical analysis.

Disclosure statement

The authors report no conflicts of interest.

Appendix A. Supplementary data

Supplementary data to this article can be found online at https://doi.org/10.1016/j.neurobiolaging.2018.10.004.

References

Alsop, D.C., Casement, M., de Bazelaire, C., Fong, T., Press, D.Z., 2008. Hippocampal hyperperfusion in Alzheimer's disease. Neuroimage 42, 1267–1274.

Alsop, D.C., Dai, W., Grossman, M., Detre, J.A., 2010. Arterial spin labeling blood flow MRI: its role in the early characterization of Alzheimer's disease. J. Alzheimers Dis. 20, 871–880.

Apostolova, L.G., Dutton, R.A., Dinov, I.D., Hayashi, K.M., Toga, A.W., Cummings, J.L., Thompson, P.M., 2006. Conversion of mild cognitive impairment to Alzheimer disease predicted by hippocampal atrophy maps. Arch. Neurol. 63, 693–699.

Badhwar, A., Tam, A., Dansereau, C., Badhwar, A., Tam, A., Dansereau, C., Orban, P., Hoffstaedter, F., Bellec, P., 2017. Resting-state network dysfunction in Alzheimer's disease: a systematic review and meta-analysis. Alzheimer's Dement. 8, 73–85.

Barker, G.R., Bird, F., Alexander, V., Warburton, E.C., 2007. Recognition memory for objects, place, and temporal order: a disconnection analysis of the role of the medial prefrontal cortex and perirhinal cortex. J. Neurosci. 27, 2948–2957.

Bondi, M.W., Houston, W.S., Eyler, L.T., Brown, G.G., 2005. fMRI evidence of compensatory mechanisms in older adults at genetic risk for Alzheimer disease. Neurology 64, 501–508.

Braak, E., Braak, H., Mandelkow, E.M., 1994. A sequence of cytoskeleton changes related to the formation of neurofibrillary tangles and neuropil threads. Acta Neuropathologica 87, 554–557.

Braak, H., Feldengut, S., Del Tredici, K., 2013. Pathogenesis and prevention of Alzheimer's disease: when and in what way does the pathological process begin? Der. Nervenarzt. 84, 477–482.

Buckner, R.L., Krienen, F.M., Castellanos, A., Diaz, J.C., Yeo, B.T., 2011. The organization of the human cerebellum estimated by intrinsic functional connectivity. J. Neurophysiol. 106, 2322–2345.

Buckner, R.L., Snyder, A.Z., Shannon, B.J., LaRossa, G., Sachs, R., Fotenos, A.F., Sheline, Y.I., Klunk, W.E., Mathis, C.A., Morris, J.C., Mintun, M.A., 2005. Molecular, structural, and functional characterization of Alzheimer's disease: evidence for a relationship between default activity, amyloid, and memory. J. Neurosci. 25, 7709–7717.

Busse, A., Hensel, A., Guhne, U., Busse, A., Hensel, A., Gühne, U., Angermeyer, M.C., Riedel-Heller, S.G., 2006. Mild cognitive impairment: long-term course of four clinical subtypes. Neurology 67, 2176–2185.

Cabeza, R., Grady, C.L., Nyberg, L., McIntosh, A.R., Tulving, E., Kapur, S., Jennings, J.M., Houle, S., Craik, F.I., 1997. Age-related differences in neural activity during memory encoding and retrieval: a positron emission tomography study. J. Neurosci. 17, 391–400.

Canto, C.B., Wouterlood, F.G., Witter, M.P., 2008. What does the anatomical organization of the entorhinal cortex tell us? Neural. Plast. 2008, 381243.

Canuet, L., Pusil, S., Lopez, M.E., Bajo, R., Pineda-Pardo, J.Á., Cuesta, P., Gálvez, G., Gaztelu, J.M., Lourido, D., García-Ribas, G., Maestú, F., 2015. Network disruption and cerebrospinal fluid amyloid-beta and phospho-tau levels in mild cognitive impairment. J. Neurosci. 35, 10325–10330.

Cope, T.E., Rittman, T., Borchert, R.J., Jones, P.S., Vatansever, D., Allinson, K., Passamonti, L., Vazquez Rodriguez, P., Bevan-Jones, W.R., O'Brien, J.T., Rowe, J.B., 2018. Tau burden and the functional connectome in Alzheimer's disease and progressive supranuclear palsy. Brain 141, 550–567.

Dai, W., Lopez, O.L., Carmichael, O.T., Becker, J.T., Kuller, L.H., Gach, H.M., 2009. Mild cognitive impairment and Alzheimer's disease: patterns of altered cerebral blood flow at MR imaging. Radiology 250, 856–866.

Das, S.R., Pluta, J., Mancuso, L., Kliot, D., Orozco, S., Dickerson, B.C., Yushkevich, P.A., Wolk, D.A., 2013. Increased functional connectivity within medial temporal lobe in mild cognitive impairment. Hippocampus 23, 1–6.

Davis, S.W., Dennis, N.A., Daselaar, S.M., Fleck, M.S., Cabeza, R., 2008. Que PASA? The posterior-anterior shift in aging. Cereb. Cortex 18, 1201–1209.

Desikan, R.S., Segonne, F., Fischl, B., Quinn, B.T., Dickerson, B.C., Blacker, D., Buckner, R.L., Dale, A.M., Maguire, R.P., Hyman, B.T., Albert, M.S., 2006. An automated labeling system for subdividing the human cerebral cortex on MRI scans into gyral based regions of interest. Neuroimage 31, 968–980.

Dickerson, B.C., Sperling, R.A., 2008. Functional abnormalities of the medial temporal lobe memory system in mild cognitive impairment and Alzheimer's disease: insights from functional MRI studies. Neuropsychologia 46, 1624–1635.

Drzezga, A., Becker, J.A., Van Dijk, K.R., Drzezga, A., Becker, J.A., Van Dijk, K.R., Sreenivasan, A., Talukdar, T., Sullivan, C., Schultz, A.P., Sepulcre, J., Putcha, D., Greve, D., Johnson, K.A., Sperling, R.A., 2011. Neuronal dysfunction and disconnection of cortical hubs in non-demented subjects with elevated amyloid burden. Brain 134, 1635–1646.

Eichenbaum, H., 2017. Memory: organization and control. Annu. Rev. Psychol. 68, 19–45.

Elman, J.A., Madison, C.M., Baker, S.L., Vogel, J.W., Marks, S.M., Crowley, S., O'Neil, J.P., Jagust, W.J., 2016. Effects of beta-amyloid on resting state functional connectivity within and between networks reflect known patterns of regional vulnerability. Cereb. Cortex 26, 695–707.

Fabiani, M., 2012. It was the best of times, it was the worst of times: a psychophysiologist's view of cognitive aging. Psychophysiology 49, 283–304.

Ferraris, M., Ghestem, A., Vicente, A.F., Nallet-Khosrofian, L., Bernard, C., Quilichini, P.P., 2018. The nucleus reuniens controls long-range hippocampo-prefrontal gamma synchronization during slow oscillations. J. Neurosci. 38, 3026–3038.

Fischl, B., Salat, D.H., van der Kouwe, A., Makris, N., Ségonne, F., Quinn, B.T., Dale, A.M., 2004. Sequence-independent segmentation of magnetic resonance images. NeuroImage 23, S69–S84.

Folstein, M.F., Folstein, S.E., McHugh, P.R., 1975. "Mini-mental state". A practical method for grading the cognitive state of patients for the clinician. J. Psychiatr. Res. 12, 189–198.

Foster, C.M., Kennedy, K.M., Horn, M.M., Hoagey, D.A., Rodrigue, K.M., 2018. Both hyper- and hypo-activation to cognitive challenge are associated with increased beta-amyloid deposition in healthy aging: a nonlinear effect. Neuroimage 166, 285–292.

Frazzini, V., Guarnieri, S., Bomba, M., Navarra, R., Morabito, C., Mariggio, M.A., Sensi, S.L., 2016. Altered Kv2.1 functioning promotes increased excitability in hippocampal neurons of an Alzheimer's disease mouse model. Cell Death Dis. 7, e2100.

Frisoni, G.B., Jessen, F., 2018. One step towards dementia prevention. Lancet Neurol. 17, 294–295.

Gilani, A.M., Knowles, T.G., Nicol, C.J., 2014. Factors affecting ranging behaviour in young and adult laying hens. Br. Poult. Sci. 55, 127–135.

Gomez-Isla, T., Price, J.L., McKeel Jr., D.W., Morris, J.C., Growdon, J.H., Hyman, B.T., 1996. Profound loss of layer II entorhinal cortex neurons occurs in very mild Alzheimer's disease. J. Neurosci. 16, 4491–4500.

Grothe, M.J., Teipel, S.J., Alzheimer's Disease Neuroimaging I, 2016. Spatial patterns of atrophy, hypometabolism, and amyloid deposition in Alzheimer's disease correspond to dissociable functional brain networks. Hum. Brain Mapp. 37, 35–53.

Grundman, M., Sencakova, D., Jack Jr., C.R., Petersen, R.C., Kim, H.T., Schultz, A., Weiner, M.F., DeCarli, C., DeKosky, S.T., van Dyck, C., Thomas, R.G., Thal, L.J., 2002. Brain MRI hippocampal volume and prediction of clinical status in a mild cognitive impairment trial. J. Mol. Neurosci. 19, 23–27.

Hagler Jr., D.J., Saygin, A.P., Sereno, M.I., 2006. Smoothing and cluster thresholding for cortical surface-based group analysis of fMRI data. Neuroimage 33, 1093–1103.

Hellyer, P.J., Shanahan, M., Scott, G., Wise, R.J., Sharp, D.J., Leech, R., 2014. The control of global brain dynamics: opposing actions of frontoparietal control and default mode networks on attention. J. Neurosci. 34, 451–461.

Henneman, W.J., Sluimer, J.D., Barnes, J., Van Der Flier, W.M., Sluimer, I.C., Fox, N.C., Fox, N.C., Scheltens, P., Vrenken, H., Barkhof, F., 2009. Hippocampal atrophy rates in Alzheimer disease: added value over whole brain volume measures. Neurology 72, 999–1007.

Hillary, F.G., Grafman, J.H., 2017. Injured brains and adaptive networks: the benefits and costs of hyperconnectivity. Trends Cogn. Sci. 21, 385–401.

Hoenig, M.C., Bischof, G.N., Seemiller, J., Hammes, J., Kukolja, J., Onur, Ö.A., Jessen, F., Fliessbach, K., Neumaier, B., Fink, G.R., van Eimeren, T., Drzezga, A., 2018. Networks of tau distribution in Alzheimer's disease. Brain 141, 568–581.

Huijbers, W., Mormino, E.C., Schultz, A.P., Wigman, S., Ward, A.M., Larvie, M., Amariglio, R.E., Marshall, G.A., Rentz, D.M., Johnson, K.A., Sperling, R.A., 2015. Amyloid-beta deposition in mild cognitive impairment is associated with increased hippocampal activity, atrophy and clinical progression. Brain 138, 1023–1035.

Jack Jr., C.R., Shiung, M.M., Gunter, J.L., O'Brien, P.C., Weigand, S.D., Knopman, D.S., Boeve, B.F., Ivnik, R.J., Smith, G.E., Cha, R.H., Tangalos, E.G., Petersen, R.C., 2004. Comparison of different MRI brain atrophy rate measures with clinical disease progression in AD. Neurology 62, 591–600.

Jack Jr., C.R., Bennett, D.A., Blennow, K., Carrillo, M.C., Feldman, H.H., Frisoni, G.B., Hampel, H., Jagust, W.J., Johnson, K.A., Knopman, D.S., Petersen, R.C., Scheltens, P., Sperling, R.A., Dubois, B., 2016. A/T/N: an unbiased descriptive classification scheme for Alzheimer disease biomarkers. Neurology 87, 539–547.

Johnson, K.A., Shultz, A., Betensky, R.A., Becker, J.A., Sepulcre, J., Rentz, D., Mormino, E., Chhatwal, J., Amariglio, R., Papp, K., Marshall, G., Albers, M., Mauro, S., Pepin, L., Alverio, J., Judge, K., Philiossaint, M., Shoup, T., Yokell, D., Dickerson, B., Gomez-Isla, T., Hyman, B., Vasdev, N., Sperling, R., Marshall, G., 2016. Tau positron emission tomographic imaging in aging and early Alzheimer's disease. Ann. Neurol. 79, 110–119.

Jones, D.T., Knopman, D.S., Gunter, J.L., Graff-Radford, J., Vemuri, P., Boeve, B.F., Petersen, R.C., Weiner, M.W., Jack Jr., C.R., 2016. Cascading network failure across the Alzheimer's disease spectrum. Brain 139, 547–562.

Kahn, I., Andrews-Hanna, J.R., Vincent, J.L., Snyder, A.Z., Buckner, R.L., 2008. Distinct cortical anatomy linked to subregions of the medial temporal lobe revealed by intrinsic functional connectivity. J. Neurophysiol. 100, 129–139.

Kaplan, E.G.H., Weintraub, S., 1983. The Boston naming test. Lea & Febiger, Philadelphia, PA.

Kircher, T.T., Weis, S., Freymann, K., Erb, M., Jessen, F., Grodd, W., Heun, R., Leube, D.T., 2007. Hippocampal activation in patients with mild cognitive impairment is necessary for successful memory encoding. J. Neurol. Neurosurg. Psychiatry 78, 812–818.

Koch, W., Teipel, S., Mueller, S., Buerger, K., Bokde, A.L., Hampel, H., Coates, U., Reiser, M., Meindl, T., 2010. Effects of aging on default mode network activity in resting state fMRI: does the method of analysis matter? Neuroimage 51, 280–287.

Lacy, J.W., Stark, C.E., 2012. Intrinsic functional connectivity of the human medial temporal lobe suggests a distinction between adjacent MTL cortices and hippocampus. Hippocampus 22, 2290–2302.

Levenga, J., Krishnamurthy, P., Rajamohamedsait, H., Wong, H., Franke, T.F., Cain, P., Sigurdsson, E.M., Hoeffer, C.A., 2013. Tau pathology induces loss of GABAergic interneurons leading to altered synaptic plasticity and behavioral impairments. Acta Neuropathol. Commun. 1, 34.

Libby, L.A., Ekstrom, A.D., Ragland, J.D., Ranganath, C., 2012. Differential connectivity of perirhinal and parahippocampal cortices within human hippocampal

subregions revealed by high-resolution functional imaging. J. Neurosci. 32, 6550–6560.
Lo, R.Y., Jagust, W.J., Alzheimer's Disease Neuroimaging Initiative, 2013. Effect of cognitive reserve markers on Alzheimer pathologic progression. Alzheimer Dis. Assoc. Disord. 27, 343–350.
Mitchell, A.J., Shiri-Feshki, M., 2009. Rate of progression of mild cognitive impairment to dementia–meta-analysis of 41 robust inception cohort studies. Acta Psychiatr. Scand. 119, 252–265.
Mohs, R.C., Cohen, L., 1988. Alzheimer's disease assessment scale (ADAS). Psychopharmacol. Bull. 24, 627–628.
Mohs, R.C., Knopman, D., Petersen, R.C., Ferris, S.H., Ernesto, C., Grundman, M., Sano, M., Bieliauskas, L., Geldmacher, D., Clark, C., Thal, L.J., 1997. Development of cognitive instruments for use in clinical trials of antidementia drugs: additions to the Alzheimer's Disease Assessment Scale that broaden its scope. The Alzheimer's Disease Cooperative Study. Alzheimer Dis. Assoc. Disord. 11 (Suppl 2), S13–S21.
Mormino, E.C., Smiljic, A., Hayenga, A.O., Onami, S.H., Greicius, M.D., Rabinovici, G.D., Janabi, M., Baker, S.L., Yen, I.V., Madison, C.M., Miller, B.L., Jagust, W.J., 2011. Relationships between beta-amyloid and functional connectivity in different components of the default mode network in aging. Cereb. Cortex 21, 2399–2407.
Morris, J.C., 1993. The Clinical Dementia Rating (CDR): current version and scoring rules. Neurology 43, 2412–2414.
Morris, J.C., Heyman, A., Mohs, R.C., Hughes, J.P., van Belle, G., Fillenbaum, G., Mellits, E.D., Clark, C., 1989. The Consortium to Establish a Registry for Alzheimer's disease (CERAD). Part I. Clinical and neuropsychological assessment of Alzheimer's disease. Neurology 39, 1159–1165.
Mueller, S.G., Schuff, N., Yaffe, K., Madison, C., Miller, B., Weiner, M.W., 2010. Hippocampal atrophy patterns in mild cognitive impairment and Alzheimer's disease. Hum. Brain Mapp. 31, 1339–1347.
Mutlu, J., Landeau, B., Gaubert, M., de La Sayette, V., Desgranges, B., Chételat, G., 2017. Distinct influence of specific versus global connectivity on the different Alzheimer's disease biomarkers. Brain 140, 3317–3328.
Nasreddine, Z.S., Phillips, N.A., Bedirian, V., Charbonneau, S., Whitehead, V., Collin, I., Cummings, J.L., Chertkow, H., 2005. The Montreal Cognitive Assessment, MoCA: a brief screening tool for mild cognitive impairment. J. Am. Geriatr. Soc. 53, 695–699.
Oh, H., Jagust, W.J., 2013. Frontotemporal network connectivity during memory encoding is increased with aging and disrupted by beta-amyloid. J. Neurosci. 33, 18425–18437.
Ossenkoppele, R., Schonhaut, D.R., Schöll, M., Lockhart, S.N., Ayakta, N., Baker, S.L., O'Neil, J.P., Janabi, M., Lazaris, A., Cantwell, A., Vogel, J., Santos, M., Miller, Z.A., Bettcher, B.M., Vossel, K.A., Kramer, J.H., Gorno-Tempini, M.L., Miller, B.L., Jagust, W.J., Rabinovici, G.D., 2016. Tau PET patterns mirror clinical and neuroanatomical variability in Alzheimer's disease. Brain 139 (pt 5), 1551–1567.
Palop, J.J., Mucke, L., 2016. Network abnormalities and interneuron dysfunction in Alzheimer disease. Nat. Rev. Neurosci. 17, 777–792.
Palmqvist, S., Scholl, M., Strandberg, O., Mattsson, N., Stomrud, E., Zetterberg, H., Blennow, K., Landau, S., Jagust, W., Hansson, O., 2017. Earliest accumulation of beta-amyloid occurs within the default-mode network and concurrently affects brain connectivity. Nat. Commun. 8, 1214.
Park, D.C., Reuter-Lorenz, P., 2009. The adaptive brain: aging and neurocognitive scaffolding. Annu. Rev. Psychol. 60, 173–196.
Pasquini, L., Scherr, M., Tahmasian, M., Meng, C., Myers, N.E., Ortner, M., Muhlau, M., Kurz, A., Forstl, H., Zimmer, C., Grimmer, T., Wohlschlager, A.M., Riedl, V., Sorg, C., 2015. Link between hippocampus' raised local and eased global intrinsic connectivity in AD. Alzheimers Dement. 11, 475–484.
Petersen, R.C., Aisen, P.S., Beckett, L.A., Donohue, M.C., Gamst, A.C., Harvey, D.J., Jack Jr., C.R., Jagust, W.J., Shaw, L.M., Toga, A.W., Trojanowski, J.Q., Weiner, M.W., 2010. Alzheimer's disease neuroimaging initiative (ADNI): clinical characterization. Neurology 74, 201–209.
Pfeffer, R.I., Kurosaki, T.T., Harrah Jr., C.H., Chance, J.M., Filos, S., 1982. Measurement of functional activities in older adults in the community. J. Gerontol. 37, 323–329.
Preston, A.R., Eichenbaum, H., 2013. Interplay of hippocampus and prefrontal cortex in memory. Curr. Biol. 23, 764–773.
Putcha, D., Brickhouse, M., O'Keefe, K., Sullivan, C., Rentz, D., Marshall, G., Dickerson, B., Sperling, R., 2011. Hippocampal hyperactivation associated with cortical thinning in Alzheimer's disease signature regions in non-demented elderly adults. J. Neurosci. 31, 17680–17688.
Ranganath, C., Ritchey, M., 2012. Two cortical systems for memory-guided behaviour. Nat. Rev. Neurosci. 13, 713–726.
Rey, A. (Ed.), 1964. L'examen clinique en psychologie. Presses Universitaires de France, Paris.
Reuter-Lorenz, P.A., Park, D.C., 2014. How does it STAC up? Revisiting the scaffolding theory of aging and cognition. Neuropsychol. Rev. 24, 355–370.
Schindler, S.E., Gray, J.D., Gordon, B.A., Xiong, C., Batrla-Utermann, R., Quan, M., Wahl, S., Benzinger, T.L.S., Holtzman, D.M., Morris, J.C., Fagan, A.M., 2018. Cerebrospinal fluid biomarkers measured by Elecsys assays compared to amyloid imaging. Alzheimers Dement. https://doi.org/10.1016/j.jalz.2018.01.013. [Epub ahead of print].
Schmitz, J.M., Green, C.E., Hasan, K.M., Vincent, J., Suchting, R., Weaver, M.F., Moeller, F.G., Narayana, P.A., Cunningham, K.A., Dineley, K.T., Lane, S.D., 2017. PPAR-gamma agonist pioglitazone modifies craving intensity and brain white matter integrity in patients with primary cocaine use disorder: a double-blind randomized controlled pilot trial. Addiction 112, 1861–1868.
Schneider-Garces, N.J., Gordon, B.A., Brumback-Peltz, C.R., Shin, E., Lee, Y., Sutton, B.P., Maclin, E.L., Gratton, G., Fabiani, M., 2010. Span, CRUNCH, and beyond: working memory capacity and the aging brain. J. Cogn. Neurosci. 22, 655–669.
Schobel, S.A., Chaudhury, N.H., Khan, U.A., Paniagua, B., Styner, M.A., Asllani, I., Inbar, B.P., Corcoran, C.M., Lieberman, J.A., Moore, H., Small, S.A., 2013. Imaging patients with psychosis and a mouse model establishes a spreading pattern of hippocampal dysfunction and implicates glutamate as a driver. Neuron 78, 81–93.
Scholl, M., Lockhart, S.N., Schonhaut, D.R., O'Neil, J.P., Janabi, M., Ossenkoppele, R., Baker, S.L., Vogel, J.W., Faria, J., Schwimmer, H.D., Rabinovici, G.D., Jagust, W.J., 2016. PET imaging of tau deposition in the aging human brain. Neuron 89, 971–982.
Schultz, A.P., Chhatwal, J.P., Hedden, T., Mormino, E.C., Hanseeuw, B.J., Sepulcre, J., Huijbers, W., LaPoint, M., Buckley, R.F., Johnson, K.A., Sperling, R.A., 2017. Phases of hyperconnectivity and hypoconnectivity in the default mode and salience networks track with amyloid and tau in clinically normal individuals. J. Neurosci. 37, 4323–4331.
Scimeca, J.M., Badre, D., 2012. Striatal contributions to declarative memory retrieval. Neuron 75, 380–392.
Sepulcre, J., Sabuncu, M.R., Li, Q., El Fakhri, G., Sperling, R., Johnson, K.A., 2017. Tau and amyloid beta proteins distinctively associate to functional network changes in the aging brain. Alzheimers Dement. 13, 1261–1269.
Sestieri, C., Shulman, G.L., Corbetta, M., 2017. The contribution of the human posterior parietal cortex to episodic memory. Nat. Rev. Neurosci. 18, 183–192.
Sperling, R.A., Laviolette, P.S., O'Keefe, K., O'Brien, J., Rentz, D.M., Pihlajamaki, M., Marshall, G., Bradley, T., Hyman, D., Selkoe, J., Hedden, T., Buckner, R.L., 2009. Amyloid deposition is associated with impaired default network function in older persons without dementia. Neuron 63, 178–188.
Sperling, R.A., Dickerson, B.C., Pihlajamaki, M., Vannini, P., LaViolette, P.S., Vitolo, O.V., Hedden, T., Becker, J.A., Dorene, M.R., Selkoe, D.J., Johnson, K.A., 2010. Functional alterations in memory networks in early Alzheimer's disease. Neuromolecular Med. 12, 27–43.
Sperling, R., Mormino, E., Johnson, K., 2014. The evolution of preclinical Alzheimer's disease: implications for prevention trials. Neuron 84, 608–622.
Spreen, O., Strauss, E., 1998. Compendium of Neuropsychological Tests. Oxford University Press, New York.
Stoodley, C.J., 2012. The cerebellum and cognition: evidence from functional imaging studies. Cerebellum 11, 352–365.
Tabatabaei-Jafari, H., Shaw, M.E., Cherbuin, N., 2015. Cerebral atrophy in mild cognitive impairment: a systematic review with meta-analysis. Alzheimers Dement. 1, 487–504.
Tulving, E., Kapur, S., Craik, F.I., Moscovitch, M., Houle, S., 1994. Hemispheric encoding/retrieval asymmetry in episodic memory: positron emission tomography findings. Proc. Natl. Acad. Sci. U. S. A. 91, 2016–2020.
van den Heuvel, M.P., Sporns, O., 2011. Rich-club organization of the human connectome. J. Neurosci. 31, 15775–15786.
Vann, S.D., Aggleton, J.P., Maguire, E.A., 2009. What does the retrosplenial cortex do? Nat. Rev. Neurosci. 10, 792–802.
Wechsler, D., 1987. WMS-R Wechsler Memory Scale–revised. The Psychological Corporation Harcourt Brace Jovanovich, San Antonio.
Wolk, D.A., Dunfee, K.L., Dickerson, B.C., Aizenstein, H.J., DeKosky, S.T., 2011. A medial temporal lobe division of labor: insights from memory in aging and early Alzheimer disease. Hippocampus 21, 461–466.
Yassa, M.A., Muftuler, L.T., Stark, C.E., 2010a. Ultrahigh-resolution microstructural diffusion tensor imaging reveals perforant path degradation in aged humans in vivo. Proc. Natl. Acad. Sci. U. S. A. 107, 12687–12691.
Yassa, M.A., Stark, S.M., Bakker, A., Albert, M.S., Gallagher, M., Stark, C.E., 2010b. High-resolution structural and functional MRI of hippocampal CA3 and dentate gyrus in patients with amnestic Mild Cognitive Impairment. Neuroimage 51, 1242–1252.
Yassa, M.A., Mattfeld, A.T., Stark, S.M., Stark, C.E., 2011. Age-related memory deficits linked to circuit-specific disruptions in the hippocampus. Proc. Natl. Acad. Sci. U. S. A. 108, 8873–8878.
Yeo, B.T., Krienen, F.M., Sepulcre, J., Sabuncu, M.R., Lashkari, D., Hollinshead, M., Roffman, J.L., Smoller, J.W., Zöllei, L., Polimeni, J.R., Fischl, B., Liu, H., Buckner, R.L., 2011. The organization of the human cerebral cortex estimated by intrinsic functional connectivity. J. Neurophysiol. 106, 1125–1165.
Yu, W., Krook-Magnuson, E., 2015. Cognitive collaborations: bidirectional functional connectivity between the cerebellum and the Hippocampus. Front. Syst. Neurosci. 9, 177.
Yushkevich, P.A., Pluta, J.B., Wang, H., Xie, L., Ding, S.L., Gertje, E.C., Mancuso, L., Kliot, D., Das, S.R., Wolk, D.A., 2015. Hippocampal Subfields Group (HSG). Automated volumetry and regional thickness analysis of hippocampal subfields and medial temporal cortical structures in mild cognitive impairment. Hum. Brain Mapp. 36, 258–287.